

# Cepheids in Open Clusters: An 8-D All-sky Census<sup>\*,†</sup>

Richard I. Anderson<sup>1,†</sup>, Laurent Eyer<sup>1</sup>, and Nami Mowlavi<sup>1</sup>

<sup>1</sup> *Observatoire de Genève, Université de Genève, 51 Ch. des Maillettes, CH-1290 Versoix, Switzerland*

27 November 2024

## ABSTRACT

Cepheids in open clusters (cluster Cepheids: CCs) are of great importance as zero-point calibrators of the Galactic Cepheid period-luminosity relationship (PLR).

We perform an 8-dimensional all-sky census that aims to identify new *bona-fide* CCs and provide a ranking of membership confidence for known CC candidates according to membership probabilities. The probabilities are computed for combinations of known Galactic open clusters and classical Cepheid candidates, based on spatial, kinematic, and population-specific membership constraints. Data employed in this analysis are taken largely from published literature and supplemented by a year-round observing program on both hemispheres dedicated to determining systemic radial velocities of Cepheids.

In total, we find 23 *bona-fide* CCs, 5 of which are candidates identified for the first time, including an overtone-Cepheid member in NGC 129. We discuss a subset of CC candidates in detail, some of which have been previously mentioned in the literature. Our results indicate unlikely membership for 7 Cepheids that have been previously discussed in terms of cluster membership.

We furthermore revisit the Galactic PLR using our *bona fide* CC sample and obtain a result consistent with the recent calibration by Turner (2010). However, our calibration remains limited mainly by cluster uncertainties and the small number of long-period calibrators.

In the near future, Gaia will enable our study to be carried out in much greater detail and accuracy, thanks to data homogeneity and greater levels of completeness.

**Key words:** methods: data analysis, catalogs, astronomical data bases: miscellaneous, stars: variables: Cepheids, open clusters and associations: general, distance scale

## 1 INTRODUCTION

The search for Cepheids in Galactic open clusters (CCs) has been a topic of interest in astronomy for the past 60 years, owing largely to their importance as calibrators of the Cepheid period-luminosity relation (PLR), discovered a

century ago among 25 periodic variable stars in the SMC by Leavitt & Pickering (1912).

The proportionality between the logarithm of Cepheid pulsation periods and their absolute magnitudes, i.e., their (logarithmic) luminosities, gives access to distance determinations and has established period-luminosity relationships as cornerstones of the astronomical distance scale (e.g. Freedman et al. 2001; Sandage et al. 2006). For reviews on Cepheids as distance indicators, cf. Feast (1999); Sandage & Tammann (2006), for instance.

The existence of the Cepheid PLR is most obvious among Cepheids in the Magellanic Clouds (e.g. Udalski et al. 1999; Soszynski et al. 2008, 2010), due to common distances (small dispersion), large statistics (thousands), and relative proximity (detectability). However, knowledge of the zero-point(s) of such relations is also required; in this case, the distances to the Magellanic Clouds. For such zero-point calibrations, PLR-independent distance estimates are required, e.g. from trigonometric parallaxes (Feast & Catchpole 1997; Benedict et al. 2007), Baade-

\* Based on observations collected at the ESO La Silla Observatory with the CORALIE échelle spectrograph mounted to the Swiss 1.2m Euler telescope.

† Based on observations obtained with the HERMES spectrograph, which is supported by the Fund for Scientific Research of Flanders (FWO), Belgium, the Research Council of K.U. Leuven, Belgium, the Fonds National Recherches Scientifique (FNRS), Belgium, the Royal Observatory of Belgium, the Observatoire de Genève, Switzerland and the Thüringer Landessternwarte Tautenburg, Germany. HERMES is mounted to the Mercator Telescope, operated on the island of La Palma by the Flemish Community, at the Spanish Observatorio del Roque de los Muchachos of the Instituto de Astrofísica de Canarias.

‡ E-mail: richard.anderson@unige.ch

Wesselink-type methods (Gieren et al. 1997; Storm et al. 2011), or objects located at comparable distance, e.g. water masers (Macri et al. 2006) or open clusters (Turner et al. 2010).

For open clusters, distances can be determined via zero-age Main Sequence or isochrone fitting. If membership can be assumed at high confidence, the cluster provides the independent estimation of the Cepheid’s distance. Confidence in cluster membership is thus critical for such calibrations.

Since the first discovery of CCs by Irwin (1955, identified SNor in NGC 6087 and USgr in M 25) and Feast (1957, established membership via radial velocities), many researchers have contributed to this field, e.g. Kholopov (1956); van den Bergh (1957); Efremov (1964); Tsarevsky et al. (1966); Turner (1986); Turner et al. (1993); Baumgardt et al. (2000); Hoyle et al. (2003); An et al. (2007); Majaess et al. (2008); Turner (2010). Nevertheless, relatively few *bona-fide* CCs (< 30) have thus far been discovered.

We therefore carry out an all-sky census of classical Cepheids in Galactic Open Clusters that aims to increase the number of *bona-fide* CCs and allows us to rank confidence in membership according to membership probabilities. Our approach is 8 dimensional in the sense that 3 spatial, 3 kinematic, and two population parameters (iron abundance and age) are used as membership constraints. Both data inhomogeneity and incompleteness are critical limitations to this work, and are acknowledged in the relevant sections. We describe our analysis in Sec. 2.

For the first time, we systematically search for cluster members among Cepheid candidates from surveys such as ASAS, NSVS, ROTSE, and also from the suspected variables in the General Catalog of Variable Stars. Most data employed to do so are taken from published catalogs or other literature. However, we also perform radial velocity observations of Cepheids on both hemispheres and determine systemic velocities,  $v_\gamma$ . To improve sensitivity to binarity, literature RVs are added to the new observations. The data compilation is described in Sec. 3.1.

The results of our census are presented in Sec. 4, starting with cluster-Cepheid combinations (Combos) that were previously studied with respect to membership, see Tab. 1 in Sec. 4.1, and followed by Combos highlighted by our work, see Tab. 2 in Sec. 4.2. The full table containing all Combos investigated in this work is provided in digital form in the online appendix and via the CDS<sup>1</sup>. An example of the information provided can be found in Tab. A2. Combos that deserve observational follow-up are identified in the text. Particular attention is given to Combos previously discussed in the literature. Discussions of additional Combos can be found in the online appendix. In Sec. 4.3, we employ our *bona-fide* CC sample in a calibration of the Galactic Cepheid PLR. The method and results are discussed in Sec. 5, which is followed by the conclusion in Sec. 6.

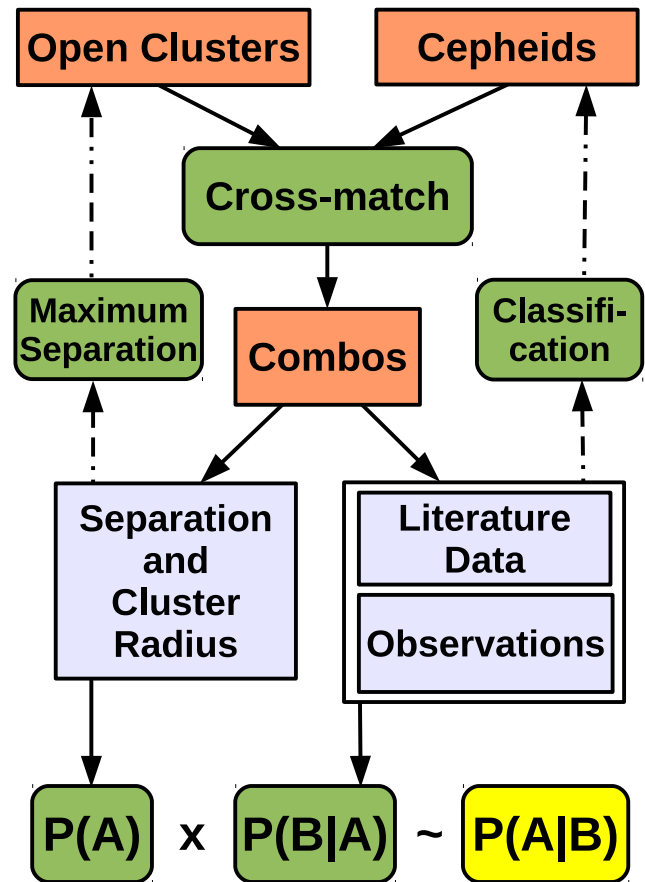


**Figure 1.** Schematic view of membership analysis. Rectangular boxes represent data sets used, green rounded boxes indicate actions. Cepheids are cross-matched (within some maximum separation) with open clusters to form Combos. Data from the literature and new observations are combined for each Combo. Cepheid classification is verified based on the data compiled (light curves, spectra). Priors,  $P(A)$ , and likelihoods,  $P(B|A)$ , are calculated separately and joined as membership probabilities,  $P(A|B)$ .

## 2 MEMBERSHIP ANALYSIS

Our all-sky census is structured as shown in Fig. 1. First, lists of known open clusters and known Cepheid candidates are compiled, see Sec. 3.1 for details. Second, the two lists are cross-matched positionally in a many-to-many relationship so that we investigate a given Cepheid’s membership in multiple different open clusters, and a given open cluster can potentially host multiple Cepheids. The correct classification of cross-matched Cepheid candidates is verified by considering light curves, and spectra. Misclassified objects are removed from the Cepheids sample. Third, membership probabilities are calculated based on all available membership constraints. These last two points are described in the present section.

Membership probabilities are calculated following Bayes’ theorem that can be formulated as (Jaynes 2003, § 4):

$$P(A|B) = \frac{P(B|A) \times P(A)}{P(B)} \propto P(B|A) \times P(A). \quad (1)$$

<sup>1</sup> <http://cds.u-strasbg.fr>

The posterior probability  $P(A|B)$  (membership probability) is proportional to the product of likelihood,  $P(B|A)$ , and prior,  $P(A)$ .  $P(B|A)$  represents the conditional probability of observing the data under the hypothesis of membership, and  $P(A)$  quantifies the degree of initial belief in membership. The normalization term  $P(B)$ , of which we possess no knowledge, is the probability to observe the data. We define  $P(A)$  in Eqs. 3 & 4 and  $P(B|A)$  in Eq. 7 below.

## 2.1 Prior Estimation and Positional Cross-match

### 2.1.1 Positional Cross-match

On-sky proximity is a necessary, but insufficient criterion for membership. Intuitively, if no other information is available, one might tentatively assume membership for a Cepheid that falls within the core radius of a potential host cluster.

Therefore, our census starts with a positional cross-match that aims to identify all combinations of cluster-Cepheid pairs that lie sufficiently close on the sky to warrant a membership probability calculation (Combos). The cross-match itself is straightforward: if the separation between a cluster's center coordinates and the Cepheid's coordinates is smaller than 2.5 degrees (to avoid unnecessary contamination), and less or equal to 5 limiting cluster radii<sup>2</sup>, we include the Combo in our analysis. Using this proximity criterion, we cross-match **990** different open clusters (of **2168** in Dias et al. 2002a) with **1021** Cepheids (of **1821** initially compiled) and obtain **3974** Combos that we investigate for membership.

The initial cross-match is purely positional, and the majority of Combos studied are non-members. Our analysis intends to weed out this majority and to indicate to us the good candidates through a high membership probability.

### 2.1.2 The Prior

We define the prior,  $P(A)$ , using the on-sky separation<sup>3</sup> between cluster center and Cepheid, weighted by the cluster radius, i.e. its apparent size on the sky.

The radius of an open cluster is typically determined by fitting an exponential radial density profile to a stellar over-density on the sky, an approach originally developed for globular clusters by King (1962). The method relies on the assumption that two separate distributions are seen: a constant field distribution and one that is attributed to the cluster.

Various ways to define cluster radii can be found in the literature. Among these are the ‘core radius’ (most stars belong to cluster),  $r_c$ , and the ‘limiting radius’ for the cluster halo (strong field star contamination),  $r_{\text{lim}}$ , see Kharchenko et al. (2005b,a) and Bukowiecki et al. (2011).

Intuitively, the probability of membership is related to separation and cluster radius, cf. Sánchez et al. (2010). Let us therefore define the quantity  $x$  as:

<sup>2</sup> This cut-off radius was adopted to include possible members of cluster halos in the analysis, inspired by the well-known case of SZ Tau in NGC 1647.

<sup>3</sup> We avoid the term ‘distance’ when referring to the on-sky separation (in arcmin) in order to prevent confusion with radial distance (in pc)

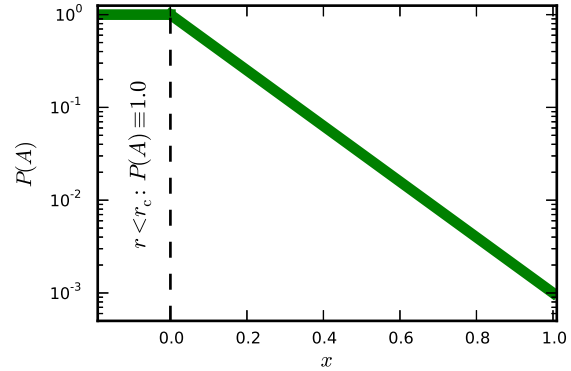


**Figure 2.** Illustration of the adopted prior,  $P(A)$ , as a function of separation normalized to a cluster's radii, expressed by the quantity  $x$ , cf. Eq. 2. If  $x \leq 0$  (Cepheid within core radius,  $r_c$ ):  $P(A) \equiv 1$ . Outside the core,  $P(A)$  decreases exponentially, inspired by radial density profiles of stars clusters. We adopt  $P(A) = 0.001$  at  $r = 2r_{\text{lim}}$ .

$$x = \frac{r - r_c}{2r_{\text{lim}} - r_c}, \quad (2)$$

where  $r$  denotes separation.  $x$  is negative, if the Cepheid lies within the cluster's (projected) core and becomes unity at a separation equal to twice the limiting radius. We define our prior,  $P(A)$ , so that (no other constraints considered) membership is assumed when the Cepheid lies within the cluster's core, i.e.  $x < 0$ . Outside  $r_c$ , inspired by radial density profiles of star clusters, we let the prior fall off exponentially and define it to reach 0.1% =  $10^{-3}$  at  $x = 1$ . Hence,

$$P(A)(x < 0) \equiv 1 \quad (3)$$

$$P(A)(x \geq 0) \equiv 10^{-3x}. \quad (4)$$

Figure 2 serves to illustrate this definition. The prior thus carries the 2-dimensional information of separation and cluster radius, and thereby takes into account how concentrated a cluster is on the sky assuming circularly distributed member stars.

## 2.2 The Likelihood $P(B|A)$

The likelihood,  $P(B|A)$ , is computed as a hypothesis test. It estimates the probability that the observed data is consistent with the null hypothesis of (true) membership. This approach was inspired by the Hipparcos astrometry-based studies by Robichon et al. (1999) and Baumgardt et al. (2000). We extend it here to take into account up to 6 dimensions using parallax,  $\varpi$ , radial velocity (RV), proper motion,  $\mu_\alpha^*$  and  $\mu_\delta$ , iron abundance,  $[\text{Fe}/\text{H}]$ , and age (open clusters assumed to be co-eval), weighting all constraints equally.

Assuming that a given Cepheid was not used to determine a cluster's (mean) parameters, we can calculate the quantity

$$c = x^T \Sigma^{-1} x, \quad (5)$$

where  $x$  denotes the vector containing as elements the differences between the (mean) cluster and Cepheid quantities:

$$x = (\varpi_{\text{Cl}} - \varpi_{\text{Cep}}, \langle v_{r,\text{Cl}} \rangle - v_{r,\text{Cep}}, \dots). \quad (6)$$

Let  $\mathbf{C}_{\text{Cl}}$  be the covariance matrix of the cluster and  $\mathbf{C}_{\text{Cep}}$

that of the Cepheid. Let  $\Sigma$  then denote the sum of the two and  $\Sigma^{-1}$  its inverse. Since the data employed in this calculation comes from many different sources, no knowledge of correlations between the different parameters is available. We thus make the assumption of independent measurements, which results in diagonal covariance matrices containing only parameter variances. Possible correlations between Cepheid and Cluster parameters are thus assumed to be negligible. We consider this justified, since we possess no knowledge of the extent of such correlations and assume that Cepheids were not used in the determination of cluster mean values. This formulation furthermore implicitly assumes normally (Gaussian) distributed errors.

Under these assumptions  $c$  is  $\chi^2$  distributed, i.e.  $c \sim \chi^2_{N_{\text{dof}}}$ , where  $N_{\text{dof}}$  is the number of degrees of freedom equal to the length of vector  $x$ , ranging from 1 to 6.  $c$  thus depends on the number of membership constraints considered (the on-sky position is used in the prior). In cases where no membership constraints are available, i.e.  $N_{\text{dof}} = 0$ , we set  $P(B|A) \equiv 1$ .

$P(B|A)$  is obtained by calculating unity minus the p-value of  $c$ ,  $p(c)$ :

$$P(B|A) = 1 - p(c). \quad (7)$$

Since the  $\chi^2$  distribution (and therefore the p-value computed) is very sensitive to  $N_{\text{dof}}$  for small  $N_{\text{dof}}$ ,  $P(B|A)$  naturally contains information on the number of membership constraints employed.

Of course, we cannot prove the null hypothesis, only exclude it. However, by including the greatest number of the most stringent membership constraints possible, this method very effectively filters out non-members. The remaining candidates can therefore be considered *bona-fide* members, provided the constraints taken into account are sufficiently strong.

The filtering effectiveness of the likelihood strongly depends on the uncertainties adopted for the constraining quantities: the larger the error, the weaker the constraint. Conversely, the smaller the error, the more important become systematic differences between quantities measured or inferred through different techniques. Obtaining reasonable estimates of the external uncertainties is of paramount importance to the success of this work, since the data considered is inhomogeneous and listed uncertainties typically provide formal errors or estimates of precision.

For certain quantities, we therefore adopt increased error budgets that we motivate and detail in the following sections. Care is taken to avoid too large or too small error budgets, and to ensure that likelihood remains an effective membership criterion.

### 3 DATA USED TO COMPUTE LIKELIHOODS

In this section, we describe how we compile the data used for our analysis. The constraints employed are: on-sky separation, parallax, proper motion, radial velocity, and the population parameters iron abundance (as a proxy for metallicity) and age. Most data considered originates from published literature and catalogs. However, we also include radial velocity (RV) data from an extensive, year-round observation program carried out on both hemispheres. Some details on

this program are provided in Sec. 3.2.3.1. A full description, however, is out of scope for this work and will be published separately.

Very often, data on a given membership constraint can be found in different references. In such cases, a choice of which reference to prefer over the other ones has to be made. In each of the following subsections, the references mentioned first are the ones preferentially adopted. This section is divided into two parts: Sec. 3.1 dedicated to open clusters, and Sec. 3.2 to Cepheids. Stellar associations are not considered.

#### 3.1 Open Cluster Data

For open cluster data used in this work, we largely rely on the Dias et al. (2002a, from hereon: D02) catalog<sup>4</sup>, which builds partially on the WEBDA database<sup>5</sup> originally developed by Mermilliod (1988, 1995), where additional useful information, e.g. on radial velocities, can be found. D02 is an extensive “living” compilation of open cluster data that is regularly updated with the latest available information on open clusters. Thanks to this process, we can assume that the most accurate available information available for the open clusters is used in our analysis. D02 is furthermore the most complete compilation of open clusters available, so that only few potential Cepheid host clusters are missed (cf. Sec. 4.1.1).

The definition of  $P(A)$  in Eqs. 2 through 4 requires information for two types of radii, core and limiting. Since D02 lists only a single quantity, apparent diameters, we adopt core and limiting radii from other sources, see Sec. 3.1.1. Further choices made regarding cluster data are presented in the subsections concerning parallax (Sec. 3.1.2), proper motion (Sec. 3.1.3), mean radial velocity (Sec. 3.1.4), iron abundance (Sec. 3.1.5), and age (Sec. 3.1.6).

Figure 3 shows the distribution of clusters (black open circles, scale with limiting radius) and Cepheids (light star symbols) in Galactic coordinates. Clusters closely trace the disk, and no obvious gaps are present in our all-sky census.

##### 3.1.1 Cluster radii

In order to choose which literature radii to adopt, we start by investigating to what degree cluster radii are reliable quantities. To this end, we search the literature for extensive catalogs that provide both core and limiting radii. Three such studies are identified: Kharchenko et al. (2005b,a, from hereon, we refer to the combined catalog from both studies as K05), Bukowiecki et al. (2011, from hereon: B11), and Kharchenko et al. (2012, from hereon: K12). We do not include Froebrich et al. (2007) here, since we notice a suspicious correlation between  $r_c$  and  $r_{\text{lim}}$ . Note, however, that some clusters listed in K12 were originally identified by Froebrich et al. (2007).

Since many clusters in K12 were also studied by K05, we compare the three radii defined in K12 with the core

<sup>4</sup> Version V3.3, 16 January 2013

<sup>5</sup> Maintained by E. Paunzen and C. Stütz in Vienna, cf. <http://www.univie.ac.at/webda/>

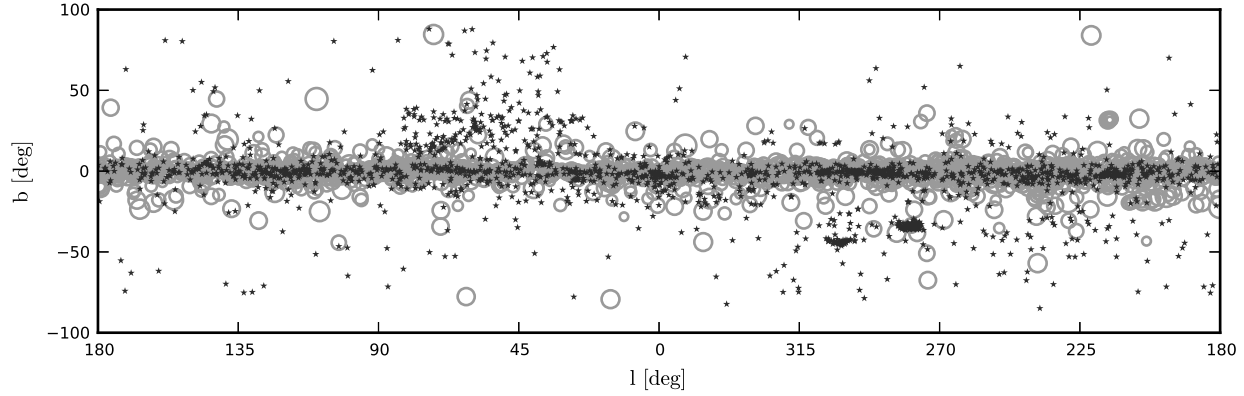


**Figure 3.** Distribution of open clusters and Cepheids compiled, shown in Galactic coordinates. Light gray open circles represent open clusters with markers logarithmically scaled for apparent size, darker gray star symbols Cepheids.

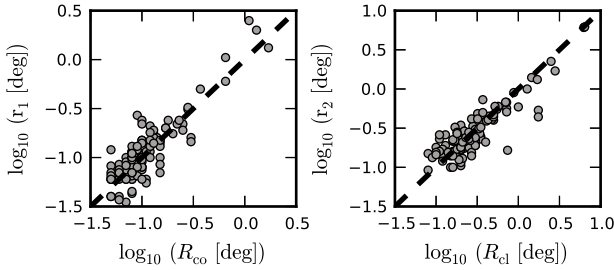


**Figure 4.** *Left panel:* comparison between  $r_1$  in K12 and the core radius,  $R_{co}$ , in K05; *right panel:* same for  $r_2$  in K12 and the limiting radius,  $R_{cl}$ , in K05. The radii are comparable.

and limiting radii in K05 and notice that the limiting radius in K05,  $R_{cl}$ , corresponds well to  $r_2$  in K12 (though  $r_2$  tends to be smaller), while  $r_1$  in K12 is rather similar to the core radius in K05,  $R_{co}$ . Nevertheless, a fair amount of scatter exists between both studies, see Fig. 4. We consider K12 an update (and extension) of K05 and therefore prefer the newer cluster parameters over the older ones.

We previously compared radii given in K05 and B11 for the clusters common to both works in Anderson et al. (2012). Rather large scatter is present (more than a factor of 2 for an appreciable fraction) and illustrates that cluster radii are subject to significant uncertainty. However, the radii from both studies follow the same trend and we therefore consider them comparable for our purpose, although K05 and K12 are based on optical and B11 on near-infrared (NIR) 2MASS (Cutri et al. 2003) photometry.

Given the sometimes rather large difference between cluster radii mentioned in the literature, we adopt a ‘permissive’ scheme that gives preference to the study giving the largest limiting radius for the cluster and thereby bias ourselves towards higher  $P(A)$ . We therefore strongly rely on the remaining membership constraints that define the likelihood to filter out chance alignments.

For 478 clusters cross-matched, only an apparent diameter was available. For these, we thus approximate  $r_c$  and  $r_{lim}$  from the typical (here: median) ratios of D02 apparent radii,  $r_{D02}$ , and the  $r_c$  and  $r_{lim}$  adopted as described above. Figure 5 illustrates this: the median ratio of  $\langle r_c/r_{D02} \rangle = 0.6$ , and  $\langle r_{lim}/r_{D02} \rangle = 2.8$ . Priors estimated using this approach

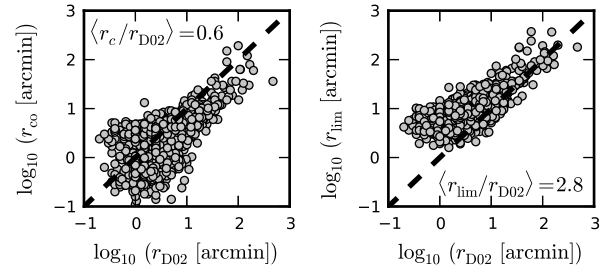


**Figure 5.** Radii based on apparent diameters from D02 compared to the core (left panel) and limiting radii (right panel) compiled from K12, K05, and B11, see text. Median ratios printed on the graph.

are identified in the online tables and marked with an asterisk in the tables presenting our results.

### 3.1.2 Cluster parallax

Distances in [pc], listed in D02, are converted to parallaxes in [mas] through Eqs. 12 and 13, see Sec. 3.2.1. Since most cluster distances listed in D02 are based on isochrone-fitting, i.e., are model dependent, we adopt an error budget of 20% to account for uncertainties arising from rotation, binarity, metallicity, and other modeling-related effects.

### 3.1.3 Mean Proper Motion

Mean cluster proper motions,  $\bar{\mu}_{\alpha, Cl}^*$  and  $\bar{\mu}_{\delta, Cl}$ , are provided in D02.

The uncertainties on mean proper motion listed in these references are typically calculated either as intrinsic dispersions (e.g. for clusters closer than approx. 400pc originally studied in K12), or as standard mean errors, i.e. the error decreases as  $\sqrt{N_* - 1}$ , where  $N_*$  is the number of stars considered members, cf. D02<sup>6</sup>. The quoted uncertainties on the cluster mean are thus much smaller than the uncertainty on an individual cluster star’s measurement. For example, in K12, the typical mean proper motion error is  $0.4 \text{ mas yr}^{-1}$ .

<sup>6</sup> See under ‘version 2.3 (25/abr/2005)’ in file: <http://www.astro.iag.usp.br/~wilton/whatsnew.txt>

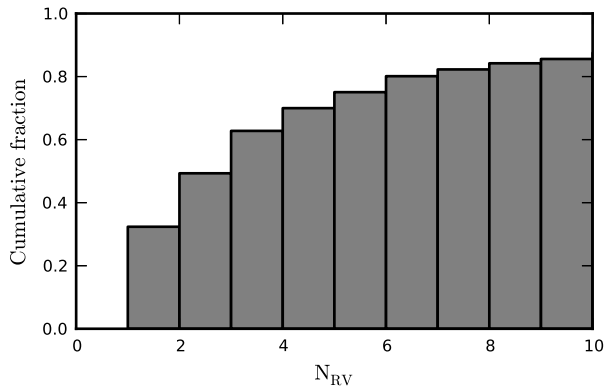


**Figure 6.** Cumulative fraction of clusters for which a given number of stars,  $N_{RV}$ , was used to determine the average RV. About half of average cluster RVs are based on a couple of stars.

For the majority of Cepheids, however, the uncertainties on proper motion are much larger, and many have been obtained from different data sets, using different techniques. Therefore, to ensure comparability of inhomogeneous data and to reduce our sensitivity to offsets in zero-points due to data-related specificities such as reduction techniques, we adopt a more generous error budget for  $\bar{\mu}_{\alpha,CI}^*$  and  $\bar{\mu}_{\delta,CI}$  that resembles the uncertainty of an individual cluster star's proper motion. This is done by multiplying the uncertainty listed by the factor  $\sqrt{N_* - 1}$  and thus slightly reduces the weight of proper motion as a membership constraint. Empirically, we are confident that this is justified, since proper motions of Cepheids typically barely exceed their uncertainties, and care should be taken not to over-interpret their accuracy.

### 3.1.4 Mean Radial Velocity

Average cluster radial velocities and associated errors are listed in D02. However, qualitative differences can exist in the uncertainties listed. For some well-studied clusters, the uncertainty given is an estimate of the intrinsic RV dispersion. For the majority of cluster RVs, however, only a few stars were used to determine the mean cluster RV (about half on two stars or less, cf. Fig. 6). These cases are therefore subject to systematic uncertainties due to implicit membership assumptions, for instance. In addition, unseen binary companions and instrumental zero-point offsets can introduce systematic uncertainties at the level of a few  $\text{km s}^{-1}$ .

We therefore adopt  $2 \text{ km s}^{-1}$  as a minimum uncertainty of the mean cluster velocity. If no uncertainty estimate is given, we adopt  $\sigma(RV_{CI}) = 10 \text{ km s}^{-1} / \sqrt{N_{RV}}$  as a typical uncertainty on the mean cluster RV, where  $N_{RV}$  is the number of stars used to determine the mean cluster RV.

### 3.1.5 Iron Abundance

We adopt iron abundances compiled in D02, including the uncertainties given. The mean uncertainty among the clusters compiled is 0.08 dex.

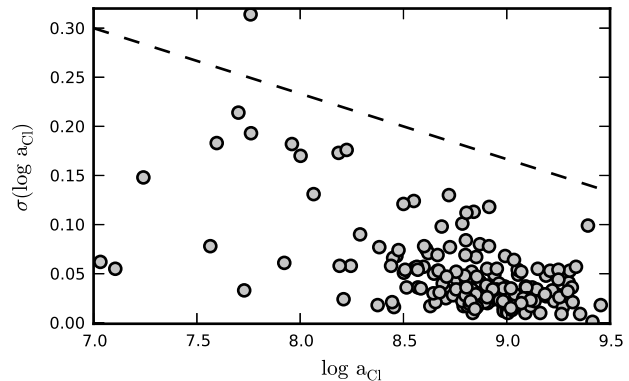


**Figure 7.** Age uncertainty,  $\sigma(\log a_{CI})$ , as function of cluster age,  $\log a_{CI}$ , given by K12. Older clusters have more precisely estimated ages. We adopt as error budget for clusters without stated age uncertainties an upper limit to this proportionality indicated by the dashed line, cf. Eq. 8.

### 3.1.6 Cluster Age

Ages were available for most clusters, since they are often determined simultaneously with the distance via isochrone-fitting. Although a model-dependent parameter, age does provide a valid constraint for membership, reflecting evolutionary considerations that are empirically validated. Quantifying an uncertainty for age as a parameter, however, is rather difficult.

Younger clusters exhibit a Main Sequence turn-off at higher stellar masses than older clusters. As a consequence of the Initial Mass Function, a younger cluster's turn-off point tends to be less populated than that of an older cluster. It therefore follows that age estimates tend to become more accurate with age, since the cluster's turn-off point tends to be defined more clearly against the field and therefore better constrains an isochrone fit.

Figure 7 corroborates the above reasoning by showing cluster ages against their uncertainties as given in K12. We thus estimate an upper limit on the uncertainty of cluster age as the dashed line in Fig. 7, which is:

$$\sigma(\log a_{CI}) \leq 0.3 - 0.067 (\log a_{CI} - 7.0) . \quad (8)$$

## 3.2 Cepheid Data

Cepheid candidates were compiled from the January 2012 version of the General Catalog of Variable Stars (Samus et al. 2012, from hereon: GCVS) and the May 2012 version of the AAVSO Variable Star Index (from hereon: VSX)<sup>7</sup>. From GCVS and VSX, we import the variability types CEP, CEP(B), DCEP, DCEPS; from VSX, we include the ASAS Pojmanski (1997, 2002); Pojmanski et al. (2005) Cepheid candidates classified as DCEP-FU or DCEP-FO. This list also contains Cepheid candidates found by ROTSE (Akerlof et al. 2000) or NSVS (Woźniak et al. 2004), as well as the ones in the suspected variables catalog (Kukarkin & Kholopov 1982).

This starting point contains an unknown, but probably

<sup>7</sup> <http://www.aavso.org/vsx/>

high, fraction of non-Cepheids. Type-II Cepheids (halo objects) and Cepheids belonging to the Magellanic Clouds are mostly removed from the sample by cross-matching with the clusters (trace the disk, see Fig. 3). To further reduce contamination, we visually inspect all ASAS-3 V-band light curves of Cepheid candidates with ASAS identifiers.

Radial pulsation and color variations during the pulsation are defining characteristics of Cepheids. We thus use the spectra obtained for radial velocity observations described in Sec. 3.2.3.1 to verify classification. A total of **151** ASAS Cepheid candidates and **32** others are thus rejected from the Cepheid sample, resulting in a final list of 1821 Cepheid candidates, **1021** of which are cross-matched with open clusters.

The cleaned sample of Cepheids cross-matched with clusters was appended with literature data from many sources, and references are given in the text. Among the most relevant references are:

- The Fernie et al. (1995) DDO Cepheid database<sup>8</sup>
- The Klagyivik & Szabados (2009) Cepheid database (KS09)
- The ASAS Catalog of Variable Stars (Pojmanski et al. 2005, ACVS) and associated photometry
- The new Hipparcos reduction (van Leeuwen 2007)
- The extended Hipparcos compilation (Anderson & Francis 2012, XHIP)
- The ASCC-2.5 catalog (Kharchenko 2001) updated by Kharchenko et al. (2007)
- The PPMXL catalog (Roeser et al. 2010)
- The 2MASS catalog (Cutri et al. 2003)
- The Cepheid photometry obtained by Berdnikov et al. (2000); Berdnikov (2008)
- The McMaster Cepheid photometry and radial velocity data archive maintained by Doug Welch<sup>9</sup>
- The radial velocity data, see Sec. 3.2.3.

### 3.2.1 Cepheid Parallaxes

Parallax,  $\varpi$ , is a key membership constraint, since cluster membership is virtually guaranteed if a Cepheid occupies the same space volume as a cluster. We combine parallax estimations from different sources, favoring *PLR-independent* determinations.

Parallax in [mas] is given preference over distance in [pc] here, since the uncertainty,  $\sigma_\varpi$ , is normally distributed, in contrast to the error in distance. This is important, since the computation of likelihoods by Eq. 7 assumes Gaussian uncertainties.

We compile parallaxes from Benedict et al. (2007, 8 Cepheids), Storm et al. (2011, 65 Cepheids), and the new Hipparcos reduction by van Leeuwen (2007, so long as  $\sigma_\varpi/\varpi \leq 0.1$  and  $\varpi > 0$ , 5 Cepheids). We then calculate PLR-based parallaxes for 622 additional Cepheids, see below.

PLR-based parallaxes of fundamental-mode Cepheids are calculated from distances computed following Turner et al. (2010). Our choice of P-L relation was motivated mainly by the considerations that i) V-band

magnitudes can be obtained for the largest number of Cepheids; ii) the above formulation is calibrated for the Galaxy using the most recent observational results, including the HST parallaxes by Benedict et al. (2007) and the cluster Cepheids from Turner (2010).

We thus calculate PLR distances as follows:

$$5 \log d = \langle m_V \rangle - \langle M_V \rangle - A_V + 5, \quad (9)$$

where  $\langle m_V \rangle$  is the apparent mean V-band magnitude, and the average absolute V-band magnitude,  $\langle M_V \rangle$ , is obtained from the pulsation period  $P$  via:

$$\langle M_V \rangle = - (1.304 \pm 0.065) - (2.786 \pm 0.075) \log P. \quad (10)$$

Eq. 10 is valid only for fundamental-mode pulsators, no distances were estimated for overtone pulsators. The total absorption,  $A_V$ , is defined as:

$$A_V = R_V \cdot E(B - V), \quad (11)$$

with  $R_V = 3.1$  the canonical ratio of total to selective extinction (reddening law) and  $E(B - V)$  the color excess of the object, cf. Sec. 3.2.1.2. The parallax is simply:

$$\varpi = \frac{1000}{d} [\text{mas}] \quad (12)$$

with  $d$  in [pc]. The parallax uncertainty,  $\sigma_\varpi$ , is obtained considering the error budget on the distance,  $\sigma_d$ :

$$\sigma_\varpi = \frac{1000}{d^2} \cdot \sigma_d [\text{mas}]. \quad (13)$$

Thus, to estimate a Cepheid's parallax, knowledge of the PLR,  $P$ ,  $\langle m_V \rangle$ , and  $A_V$  is required. Periods are usually available in the GCVS or the VSX, whereas average magnitudes and color excesses of many of the newer Cepheid candidates are not available in the literature. However,  $E(B - V)$  can be estimated from combined NIR and optical data. The following paragraphs describe in detail how these quantities are compiled.

**3.2.1.1 Mean Magnitude,  $\langle m_V \rangle$**  We compile mean V-band magnitudes,  $\langle m_V \rangle$ , from multiple references. Different methods of determining mean magnitudes exist, and the photometry employed is inhomogeneous, forcing us to adopt a zero-point for mean magnitudes compiled. In Fig. 8 we therefore compare mean magnitudes from Klagyivik & Szabados (2009, from hereon: KS09) with the Fernie et al. (1995) database's magnitude-based means and the intensity-means from Berdnikov et al. (2000). For the Cepheids common to both studies, KS09 and the Fernie magnitudes show excellent agreement. We therefore adopt the following order of preference for compiling mean magnitudes.

First, we adopt  $\langle m_V \rangle$  values from KS09 with a fixed error budget of 0.03 mag, since the study carefully investigates amplitudes with a special focus on binarity.

Second, we adopt the magnitude-based means from the Fernie database with uncertainties calculated as the difference between intensity- and magnitude-mean magnitudes, with a minimum error of 0.03 mag.

Third, we include Berdnikov et al. (2000) mean magnitudes. As seen in Fig. 8, these  $\langle m_V \rangle$  values are systematically smaller (brighter) by approx. 0.03 mag than KS09. This discrepancy is most likely due to different ways of determining

<sup>8</sup> <http://www.astro.utoronto.ca/DDO/research/Cepheids/>

<sup>9</sup> <http://crocus.physics.mcmaster.ca/Cepheid/>



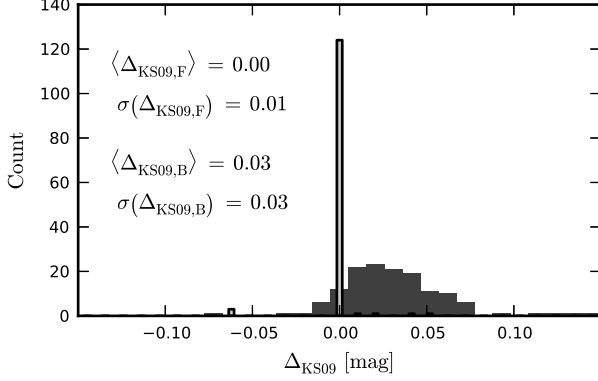


**Figure 8.** Histogram of differences in mean magnitudes relative to the KS09 values,  $\Delta_{\text{KS09}}$ . Light slim bars show  $\Delta_{\text{KS09,F}}$  computed using Fernie values (123 Cepheids); Darker broad bars with no outline show  $\Delta_{\text{KS09,B}}$  computed using data from Berdnikov et al. 2000 (127 Cepheids). Mean differences,  $\langle \Delta_{\text{KS09}} \rangle$ , and dispersions,  $\sigma(\Delta_{\text{KS09}})$ , given in [mag].

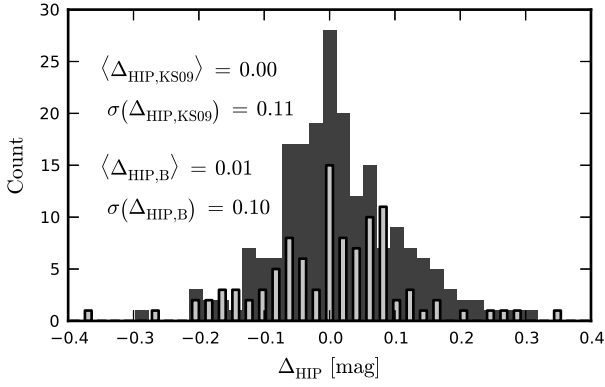


**Figure 9.** Histogram of differences in mean magnitudes relative to Hipparcos median V-band,  $\Delta_{\text{HIP}}$ . Light slim bars show  $\Delta_{\text{HIP,KS09}}$  computed using KS09 (104 Cepheids). Darker broad bars with no outline show  $\Delta_{\text{HIP,B}}$  computed using Berdnikov et al. 2000 (198 Cepheids). Mean differences,  $\langle \Delta_{\text{HIP}} \rangle$ , and dispersions,  $\sigma(\Delta_{\text{HIP}})$ , given in [mag].

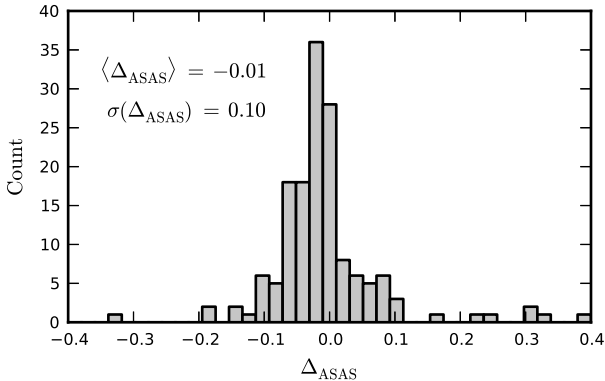


**Figure 10.** Histogram of differences in mean V-band magnitude computed from ASAS light curves for 154 Cepheids relative to reference values from Fernie and KS09,  $\Delta_{\text{ASAS}}$ , cf. also Fig. 8. Mean difference,  $\langle \Delta_{\text{ASAS}} \rangle$ , and dispersion,  $\sigma(\Delta_{\text{ASAS}})$ , given in [mag].

the mean. We remove this offset from the Berdnikov et al. (2000) values for internal consistency and adopt 0.03 mag as error budget for these values, identical to KS09.

Fourth, we employ median V-band magnitudes from the Hipparcos catalog (Perryman & ESA 1997, obtained via XHIP) for 8 Cepheids. The median V-band magnitudes derived from Hipparcos magnitudes can differ significantly from mean magnitudes listed in other references, cf. Fig. 9. Usually, this is due to contamination due to a nearby star within the instantaneous field of view. As error budget for the Hipparcos median V-magnitudes, we adopt  $\sigma(\Delta_{\text{HIP,KS09}}) = 0.110$  mag, see Fig. 9. We note that we could find no dependence on period or number of transits for this dispersion.

Fifth, we adopt average apparent V-band magnitudes that we determine from ASAS-3 light curves. To this end, we fit Fourier series (same procedure as described for radial velocities in Sec. 3.2.3.3) to the phased light curves and use the constant term as the average,  $\langle m_V \rangle$ . Figure 10 shows a histogram of  $\Delta_{\text{ASAS}}$ , the differences between the computed ASAS-based  $\langle m_V \rangle$  and Fernie or KS09. We remove the offset of  $-0.01$  mag from the ASAS mean magnitudes and adopt the dispersion of 0.10 mag computed as the error budget.

The large dispersion,  $\sigma(\Delta_{\text{ASAS}})$ , in Fig. 10 probably originates from contamination due to nearby stars. To illustrate this, Fig. 12 shows phase-folded ASAS-3 V-band light curves of two Cepheids, CY Car (left) and BM Pup (right). Our mean magnitude agrees well with the literature value for CY Car. For BM Pup however, a systematic difference of approximately 0.144 mag is evident, although the light curve appears to be clean otherwise. Inspection of a DSS images, however, reveals that contamination from a nearby companion is likely. Out of 154 Cepheids for which the ASAS light V-band curves were inspected, 20 differed by more than 0.1 mag from the reference value, and 28 agreed to within 0.01 mag.

If no mean magnitude is obtained from any of the above sources, we perform a (rough) estimate of  $\langle m_V \rangle$  based on the information provided in the GCVS and the VSX, using the magnitude at maximum brightness,  $\min_V$ , and the amplitude,  $\text{amp}_V$ , of the V-band light curve.  $\text{amp}_V$  is either provided directly by the catalogs, or calculated as the difference between minimum and maximum brightness,  $\text{amp}_V = \max_V - \min_V$ .

Since Cepheid light curves are skewed, their mean magnitudes do not necessarily lie at half the amplitude. We therefore estimate the typical fractional amplitude at mean brightness,  $\langle f_a \rangle$ , to compute  $\langle m_V \rangle = \min_V + \langle f_a \rangle \text{amp}_V$ . Figure 11 shows a histogram of  $f_a$  computed using mean magnitudes listed in the Fernie database,  $\langle m_{V,F} \rangle$ , and amplitudes,  $\text{amp}_V$ , from the catalogs. We find

$$\langle f_a \rangle \equiv \text{median} \left( \frac{\langle m_{V,F} \rangle - \max_V}{\min_V - \max_V} \right) = 0.54 \pm 0.079. \quad (14)$$

We derive an uncertainty on  $\langle m_V \rangle$  thus obtained using the uncertainty on  $\langle f_a \rangle$ , an estimated error on the amplitude, and a prescribed error on the magnitude at maximum brightness (we adopt 0.1 mag for 12th magnitude and below, and increase linearly to 0.5 mag at 20th magnitude). The resulting mean error on  $\langle m_V \rangle$  is 0.27 mag.

This estimation works reasonably well, although there exist obvious limitations, such as inhomogeneity of pass-



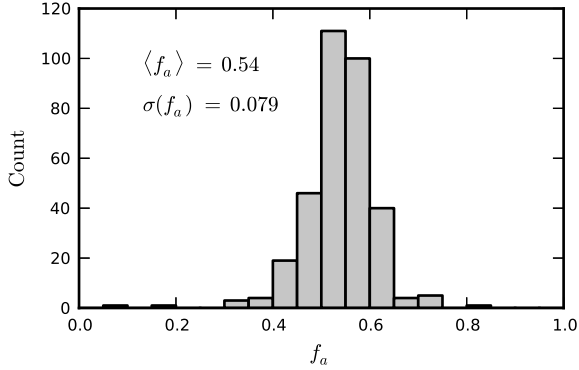


**Figure 11.** Fractional amplitudes,  $f_a$ , computed from Fernie mean, and GCVS maximum and minimum magnitudes, see Eq. 14.

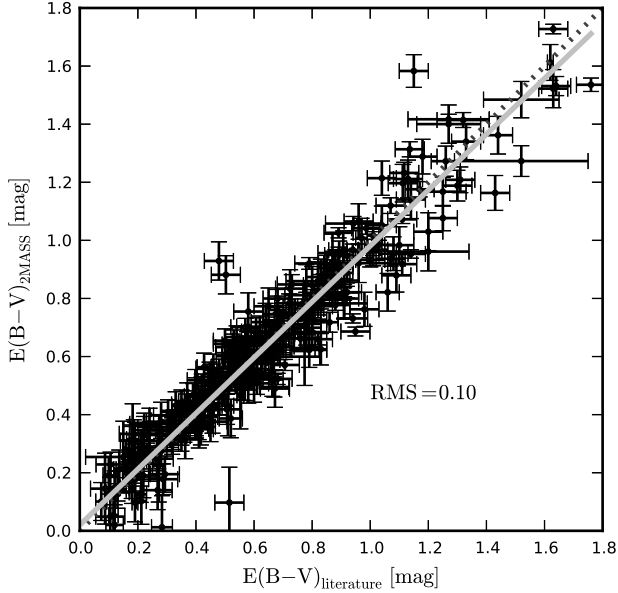


**Figure 13.** Color excess from the literature against 2MASS-based estimate. The solid line represents a weighted least squares fit, a dashed line indicates the diagonal. RMS around either line: 0.10 mag.

bands, accuracy of the upper and lower limits, the applicability of the above ratio for a given Cepheid. Nevertheless, it does provide access to rough estimates of  $\langle m_V \rangle$  for Cepheids with little available information.

Given the many different ways in which average magnitudes were estimated, we keep track of the type of estimation to ensure traceability of any potential issues.

**3.2.1.2 Color excess,  $E(B - V)$**  The principal references adopted for color excess are Kovtyukh et al. (2008); Laney & Caldwell (2007); Sziládi et al. (2007); Fouqué et al. (2007). Where available, we adopt stated uncertainties,  $\sigma(E(B - V))$ . If no  $\sigma(E(B - V))$  are listed, we adopt an error budget of 0.05 mag for Kovtyukh et al. (2008)

and Sziládi et al. (2007), and 0.03 mag for Laney & Caldwell (2007).

For other Cepheids, we adopt  $E(B - V)$  from the Fernie database and an error budget of 0.05 mag, unless the standard error from multiple reddening estimations was given.

Color excesses for Cepheids with no literature  $E(B - V)$  are estimated following Majaess et al. (2008) using mean J-band magnitudes by Monson & Pierce (2011), or single-epoch 2MASS (Cutri et al. 2003) J-band magnitudes,  $m_J(\text{JD})$ . The method requires knowledge of the pulsation period,  $P$ , and the average J-band magnitude,  $\langle m_J \rangle$ . If not known from the literature, the latter can be estimated by (Majaess et al. 2008, Eq. 5):

$$\langle m_J \rangle \simeq m_J(\text{JD}) - \left[ \frac{|m_V(\phi_J) - \text{max}_V|}{\text{amp}_V} - 0.5 \right] \cdot 0.37 \text{amp}_V, \quad (15)$$

where  $\phi_J$  denotes the pulsation phase of the J-band measurement, and  $m_V(\phi_J)$  is the V-band magnitude at that phase.  $E(B - V)$  can then be estimated by

$$E(B - V) = -0.270 \log P + 0.415 (\langle m_V \rangle - \langle m_J \rangle) - 0.255. \quad (16)$$

Wherever possible,  $m_V(\phi_J)$  was obtained from the ASAS light curve. If this is impossible, we assume a sinusoidal light curve with the given mean magnitude and (semi-)amplitude.

Uncertainties or changes in pulsation period can significantly impact the phase calculated for the single-epoch 2MASS measurement,  $\phi_J$ . We therefore optimize Cepheid ephemerides for which ASAS data were available. To do so, we compute a grid (at fixed periods) of Fourier series fits around the period provided in the ACVS and retain the solution with the minimum root mean square. Epochs are optimized by simply shifting the phase-folded curve. Figure 14 illustrates this step for the overtone Cepheid QZ Nor. We then take care to employ the most recently determined pulsation ephemerides available and estimate reddening uncertainties using error propagation for the quantities involved.

We note that this approach may be subject to multiple issues such as: i) the unknown shape of the light curve; ii) the applicability of Eq. 16; iii) period changes that impact  $m_V(\phi_J)$ ; iii) the approximate form of the relationship in Eq. 15. We therefore compare the 2MASS-based color excesses to the reference values, see Fig. 13, where the result of a weighted least squares fit is indicated by a straight line and does not differ much from the diagonal indicated by a dashed line. Despite considerable dispersion, the correspondence is clear and the results are promising (RMS of 0.1 mag).

### 3.2.2 Proper Motions

Cepheid proper motions are taken from the following sources in order of preference:

- (i) Hipparcos proper motions from the new reduction by van Leeuwen (2007)
- (ii) The PPMXL catalog by Roeser et al. (2010)

### 3.2.3 Systemic Radial Velocities

**3.2.3.1 New Observations** In order to extend the number of Cepheids with known systemic radial velocities,

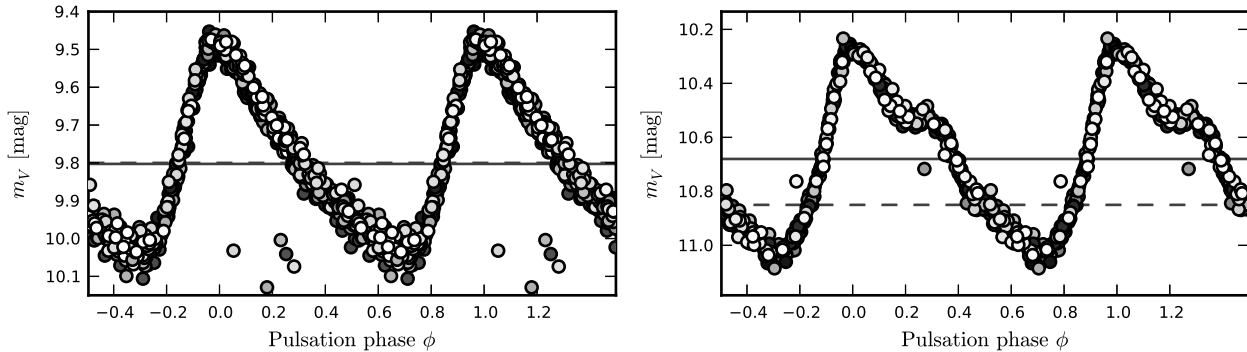


**Figure 12.** Phase-folded ASAS-3 V-band light curves of CY Car (left) and BMPup (right). Julian date of observation indicated in grayscale, increasing from black to white. Horizontal lines indicate reference average magnitude (dashed, KS09) and constant term of the fitted Fourier series (solid). For CY Car, the two are in excellent agreement. BMPup has a bright neighbor that contaminates the aperture used to measure its flux, leading to an underestimated (too bright) mean magnitude.

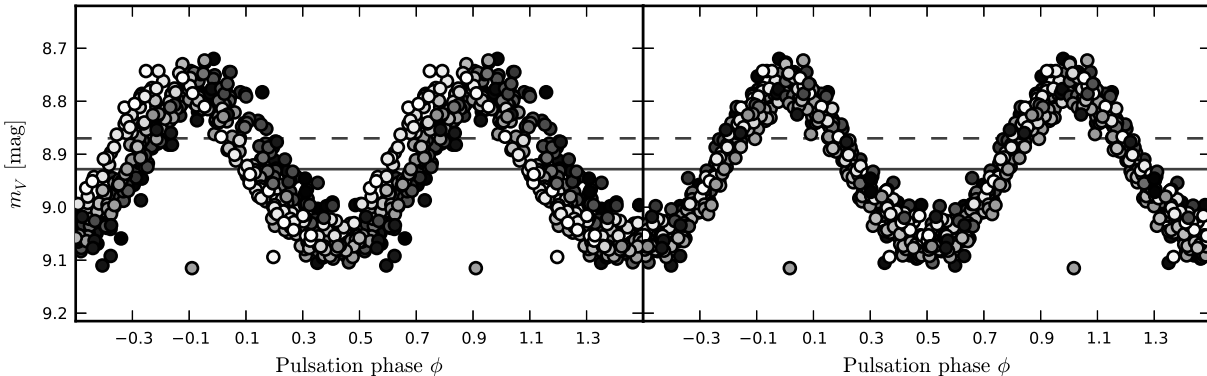


**Figure 14.** ASAS-3 V-band phase-folded light curve of QZNor. Grayscaled symbols (from black to white) indicate increasing Julian date of observation. *Left panel:* pulsation period and epoch of maximum light from the ACVS. *Right panel:* optimized period and epoch used.

$v_\gamma$ , we<sup>10</sup> carried out observations between November 2010 and July 2012 using the fiber-fed high-resolution echelle spectrographs *CORALIE* (Queloz et al. 2001, see also the instrumental upgrades described in Ségransan et al. 2010,  $R \sim 60000$ ) at the 1.2m Euler telescope at La Silla, Chile, and *HERMES* (Raskin et al. 2011,  $R \sim 80000$ ) at the identically-built Mercator telescope on La Palma. In total, we observed 103 Cepheids with *CORALIE* and 63 with *HERMES*. 18 Cepheids were observed with both instruments, i.e. from both hemispheres. For 85 of these Cepheids, no radial velocity (RV) data are available in the literature.

Efficient reduction pipelines exist for both instruments that include pre- and overscan bias correction, cosmic removal, as well as flatfielding using Halogen lamps and background modelization. ThAr lamps are used for the wavelength calibration.

The RVs are computed via the cross-correlation technique described in Baranne et al. (1996). We use numerical masks designed for solar-like stars (optimized for spectral type G2) for all cross-correlations. Both instruments are

very stable and yield very high precision RVs of  $\sim 10 \text{ ms}^{-1}$  (Queloz et al. 2000; Raskin et al. 2011). The measurement uncertainty is therefore not limited by the instrumental precision, but by line asymmetries due to pulsation. A detailed investigation of these effects is out of scope for this paper and will be presented in a future publication. The typical uncertainty on individual measurements is thus at the  $100 - 300 \text{ ms}^{-1}$  level, depending on the star and pulsation phase.

**3.2.3.2 Literature Data** In addition to the previously unpublished radial velocities described in Sec. 3.2.3.1, we employ literature data from many references to determine systemic velocities,  $v_\gamma$ , see Sec. 3.2.3.3. The addition of literature RVs extends the baseline of our otherwise relatively short (1.5 years) observing program, thereby enhancing our sensitivity to binarity. For binary Cepheids<sup>11</sup> with published orbital solutions, we adopt the literature  $v_\gamma$ .

Aside from the systemic RVs in the Fernie database and KS09, we compile RV time series from the follow-

<sup>10</sup> The authors are grateful to the observers who contributed in this effort; names are given in the acknowledgments.

<sup>11</sup> cf. L. Szabados' database of binary Cepheids available at <http://www.konkoly.hu/CEP/nagytab3.html>

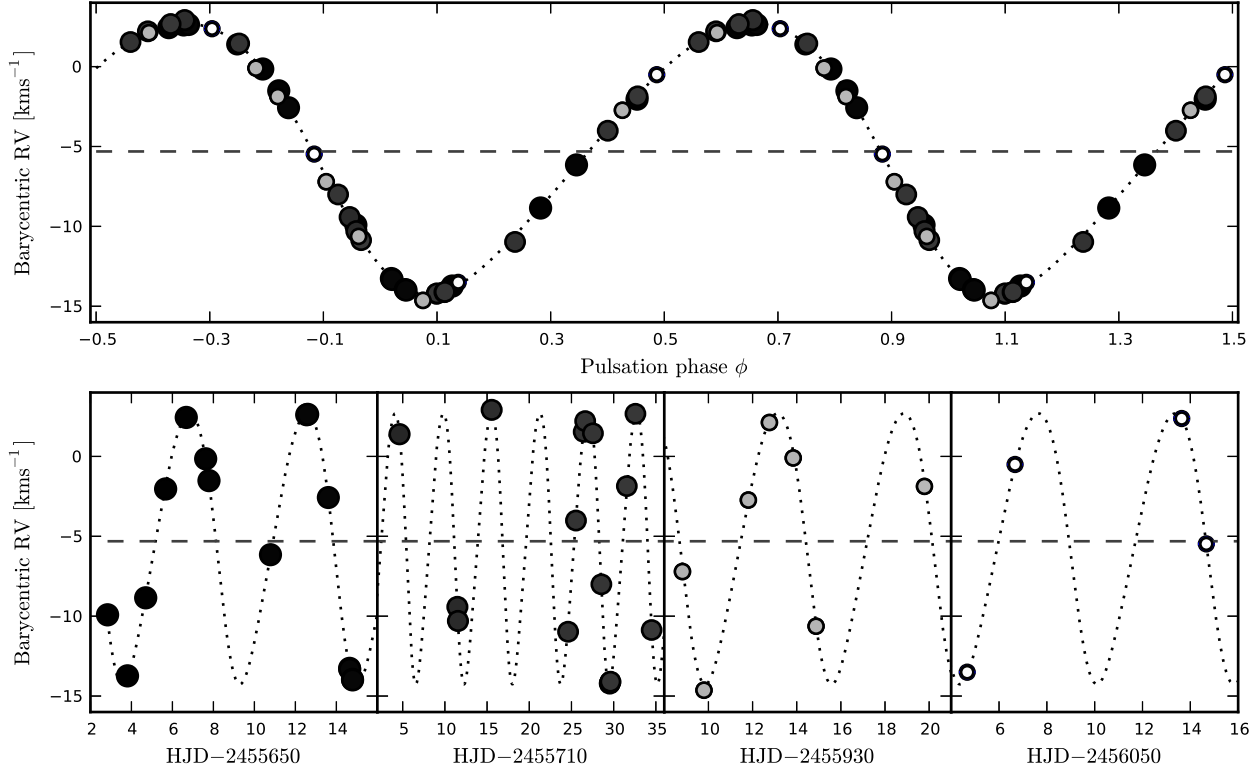


**Figure 15.** RV data recently published in Szabados et al. (2013) for first-overtone pulsator GH Car, obtained in southern hemisphere with *CORALIE* as part of our program. Grayscale (black to white) and size-code (larger to smaller) indicate increasing Julian Date of observation. Fit of triple-harmonic Fourier series indicated by a dotted line.  $v_\gamma$  indicated by a dashed horizontal line. *Top panel:* phase-folded, *Bottom panel:* non-folded, showing zooms of the four observing runs during which data were obtained.

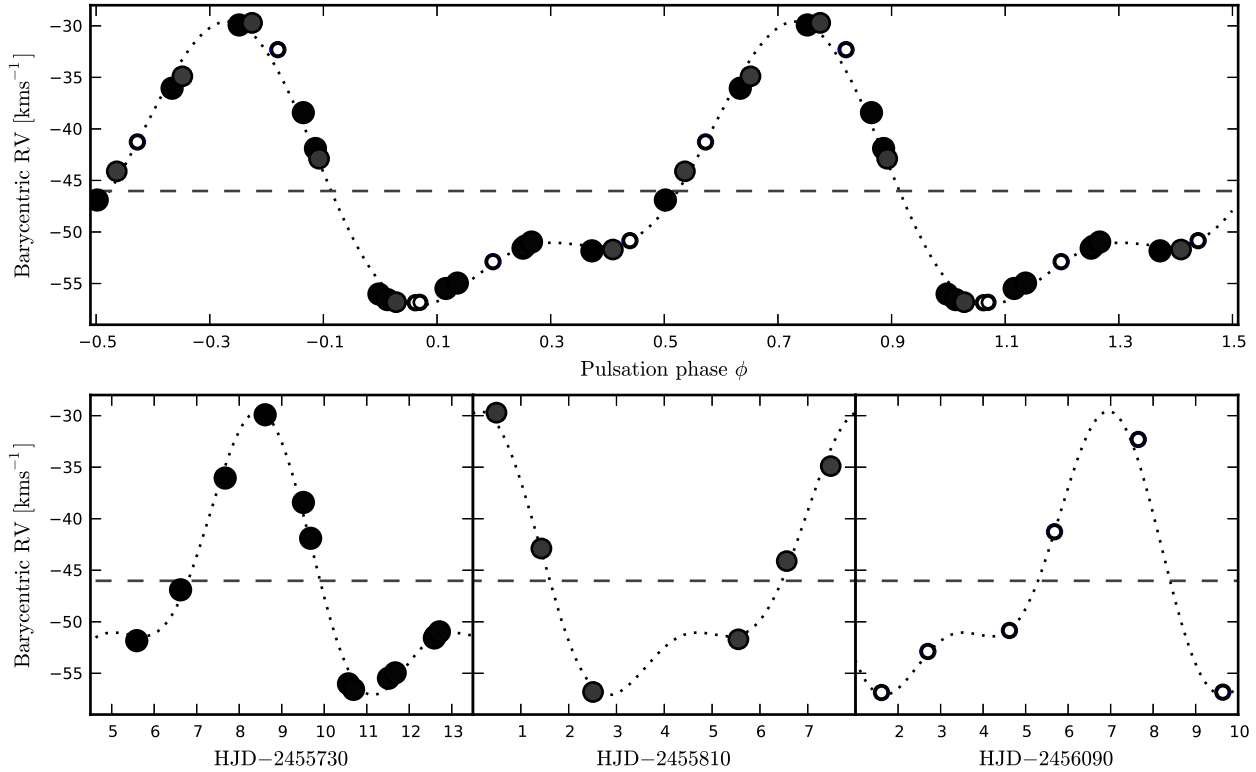


**Figure 16.** New RV data for fundamental-mode Cepheid V2340 Cyg, obtained in northern hemisphere with *HERMES*. Grayscale (black to white) and size-code (larger to smaller) indicate increasing Julian Date of observation. Fit of triple-harmonic Fourier series indicated by dotted line.  $v_\gamma$  indicated by a dashed horizontal line. *Top panel:* phase-folded, *Bottom panel:* non-folded, showing zooms of the three observing runs during which data were obtained.

ing sources: Lloyd Evans (1980); Gieren (1981, 1985); Evans (1983); Coulson et al. (1985); Coulson & Caldwell (1985); Barnes et al. (1987, 1988); Gieren et al. (1989); Wilson et al. (1989); Metzger et al. (1991, 1992, 1998); Gorynya et al. (1992, 1996, 1998, 2002); Evans & Welch (1993); Pont et al. (1994, 1997); Bersier et al. (1994); Bersier (2002); Kiss (1998); Imbert (1999); Storm et al. (2004); Barnes et al. (2005); Petterson et al. (2005); Baranowski et al. (2009). The data for most of these sources dated earlier than 1986 are extracted from the McMaster Cepheids database. Newer data are obtained through VizieR<sup>12</sup>.

**3.2.3.3 Systemic Radial Velocities,  $v_\gamma$**  The systemic radial velocity,  $v_\gamma$ , is obtained by fitting a Fourier series to the RVs. We use pulsation period,  $P$ , as a fixed parameter, since it is known for all Cepheids we observed.

The basic analytical form applied was a Fourier series with  $n$  harmonics and phase  $\phi$  is:

$$FS_n = v_\gamma + \sum_{n=1,2,3,\dots} a_n \sin(2n\pi\phi) + b_n \cos(2n\pi\phi) \quad (17)$$

Since the number of data points available varies for each star, we do not fix the number of harmonics in this fit. Instead, we iteratively increase the degree of the Fourier series until an F-test indicates an overly complex representation, i.e. when spurious fit improvement is more likely than 0.27%. For some stars, we therefore use only a simple sine function, whereas stars with many measurements are fitted using up to five harmonics. We show two examples of newly observed RV curves in Figs. 15 and 16. A full description and publication of the new radial velocity data will follow in the near future.

We adopt a fixed error budget of  $3 \text{ km s}^{-1}$  on  $v_\gamma$ . Although this may overestimate the uncertainties for some very good cases, it is intended to account for a range of systematic errors, such as unseen binarity, instrumental zero point differences and insufficient phase coverage. We are confident that this error budget is sufficiently large to prevent the exclusion of good member candidates, while being sufficiently small to provide a stringent constraint. If insufficient data points render the Fourier fit unsatisfactory, we determine a rough estimate of  $v_\gamma$  and its error budget by eye.

### 3.2.4 Iron Abundance

We rely mostly on iron abundances by Luck & Lambert (2011) and complement these with the compilation in KS09 that made the enormous effort of homogenizing iron abundances from the literature available, namely from Giridhar (1983); Fry & Carney (1997); Andrievsky et al. (2002b,a,c); Luck et al. (2003); Groenewegen et al. (2004); Andrievsky et al. (2004, 2005); Kovtyukh et al. (2005a,b); Romaniello et al. (2005); Mottini (2006); Yong et al. (2006); Lemasle et al. (2007), as well as the work by Sziládi et al. (2007); Lemasle et al. (2008); Romaniello et al. (2008).

Unfortunately, the adopted standard value of solar iron abundance can vary among references, possibly introducing

systematic offsets between different authors' studies. Furthermore, an estimation of the iron abundance in a Cepheid is more complex than in a non-pulsating star, since the stellar parameters (e.g. temperature and turbulence) vary during the pulsation cycle, and since the atmosphere is not static. We therefore adopt generous error budgets of 0.1 dex for the values from Luck & Lambert (2011), and 0.15 dex in  $[\text{Fe}/\text{H}]$  for the others.

### 3.2.5 Age

Cepheid ages can be calculated for first overtone and fundamental mode pulsators using the period-age (PA) relations given in Bono et al. (2005). For fundamental mode Cepheids, we use  $\log t = (8.31 \pm 0.08) - (0.67 \pm 0.01) \log P$ . For overtone pulsators, the relation used is  $\log t = (8.08 \pm 0.04) - (0.39 \pm 0.04) \log P$ . Age error budgets are calculated from the uncertainties stated for slope and intercept.

## 4 RESULTS

This section presents the results from our census. As mentioned in Sec. 3.1, some host Cepheid clusters known in the literature (e.g. in Turner & Burke 2002, or T10) are not present in our cluster sample. Such cases are briefly mentioned in Sec. 4.1.1. We furthermore note that stellar associations are not considered here.

In addition to the membership probabilities computed, we consider the quality of the data employed to constrain membership, and compare our results to the published literature. We then flag Combos as *bona fide*, inconclusive, unlikely, or non-members. These flags are attributed according to the following reasoning:

- *bona fide* is attributed to Combos with typically high priors and high likelihoods constrained by multiple parameters, in particular parallax. Closer inspection of the individual membership employed or the literature builds confidence in membership. Some Combos studied in detail in the literature prove to be strong candidates, despite low probabilities computed here, pointing to limitations of the data used as input in our analysis. We consider these Combos *bona fide* members.
- *inconclusive* CCs are candidates for which the membership constraints available are insufficient to consider them *bona fide*, e.g. if  $P(A) > 0.5$  with no additional membership constraints. We flag newly-identified Combos as *inconclusive*, if the prior vanishes and  $0.1 < P(B|A) < 0.8$  has been computed from at least 3 membership constraints that exceed the combined error budgets. These candidates warrant follow-up.
- *unlikely* CCs have low likelihoods ( $< 10\%$ ) due to discrepant membership constraints (more than one constraint off by approximately  $2\sigma$ ), although evidence supporting membership may exist in the literature. Membership cannot be ruled out altogether for these candidates that may benefit from additional follow-up.
- *non-members* form the majority of Combos cross-matched. They are clearly inconsistent with membership.

It should be kept in mind that our analysis is of a statistical nature may not provide the final answer for every

<sup>12</sup> <http://vizier.u-strasbg.fr/viz-bin/VizieR>

Combo. While the benefit of our analysis is a consistent and transparent approach to determining membership, the correctness of our membership probabilities relies entirely on the accuracy of the input data; this is particularly true for reddening and distances, or pulsation modes. Therefore, we caution that CCs previously discussed in the literature that are found to be unlikely or non-members by our analysis should not be discarded fully without additional consideration or follow-up.

We start the presentation of our results with CCs known from the literature (Sec. 4.1). While we take care to include relevant references, it is almost inevitable that some works are overlooked in a field with this much history. The literature CCs are followed by new candidates and other newly-identified Combos of interest (Sec. 4.2). For brevity of the main body, we defer presentation of inconclusive, unlikely, and inconsistent Combos to appendix A.

In Sec. 4.3, we then revisit the Galactic Cepheid period-luminosity relationship using our *bona fide* CC sample.

#### 4.1 Literature Combos

The main references considered for CCs are Feast (1999), Turner & Burke 2002, and Turner (2010, from hereon: T10). Additional Cepheids whose cluster membership was considered in the literature are mentioned where appropriate, cf. also the references given in the caption of Tab. 1 and Sec. 4.1.1.

Table 1 lists the CCs previously discussed in the literature that are recovered by our analysis. A horizontal line divides cases that we find can be consistent with membership according to the data compiled (above), and those that tend to be inconsistent with membership in our analysis (below). Two essentially unconstrained Combos known in the literature are included above the horizontal line. For each deviant membership constraint, i, we list the level of disagreement between cluster and Cepheid value, i.e.,  $|x_i|$  from Eq. 6, in units of the square-summed uncertainties  $\sigma_i^2 = \sigma_{Cl,i}^2 + \sigma_{Cep,i}^2$ .

##### 4.1.1 Missed Combos

Our analysis is limited to open clusters listed in D02. The following CCs reside in nearby sparse clusters that are not included in D02 and could thus not be studied by our analysis:  $\alpha$  UMi (Turner et al. 2013, but see also van Leeuwen 2013);  $\delta$  Cep (e.g. Majaess et al. 2012a);  $\zeta$  Gem (Majaess et al. 2012b); SU Cas (Majaess et al. 2012c,d; Turner et al. 2012).

##### 4.1.2 Bona-fide CCs

Based on the available data and literature, we flag the following literature Combos as *bona fide* CCs, cf. Tab. 1: USgr in IC 4725; CF Cas, CE Cas A & B in NGC 7790; DL Cas in NGC 129; SU Cyg in Turner 9; V367 Sct in NGC 6649, V340 Nor and QZ Nor in NGC 6067; TW Nor in Lynga 6; CV Mon in vdBergh 1; SNor in NGC 6087; BBSgr in Collinder 394; RU Sct in Collinder 394; CG Cas in Berkeley 58; V Cen in NGC 5662. For more information on those Combos with high priors and high likelihoods, i.e., the more or less obvious members, we refer to the original references

listed in Tab. 1, as well as to the data table supplied in electronic form. As mentioned in Sec. 4, some Combos flagged as *bona fide* CCs require inspection of the available data and literature in addition to the membership probabilities in order to conclude on membership. We discuss these combos in the paragraphs below.

**4.1.2.1 V340 Nor and QZ Nor in NGC 6067** We find two Cepheids that appear to belong to NGC 6067, namely V340 Nor, which lies within its core radius, and QZ Nor, an overtone pulsator (KS09) that lies outside  $r_{lim}$ . Cluster membership for QZ Nor was first considered by Eggen (1983), and by Walker (1985b) for V340 Nor. All membership constraints were employed for both Cepheids, and both are consistent with membership for the open cluster data listed in D02. The only discrepant constraint is age for V340 Nor.

If both Cepheids belong to the same cluster, then their respective membership constraints should agree. Interestingly, the distance estimate of QZ Nor by Storm et al. (2011) is much closer to the cluster's, while there are nearly 400pc difference between the estimates for both Cepheids. In terms of parallax, QZ Nor ( $0.74 \pm 0.07$  [mas]) is consistent with NGC 6067 ( $0.71 \pm 0.14$  [mas]), but slightly off from V340 Nor ( $0.58 \pm 0.09$  [mas]). However, the difference in  $v_\gamma$  between the two Cepheids is minimal ( $0.73 \text{ km s}^{-1}$ ). Given that V340 Nor is a visual binary, the small offset in proper motion between the two Cepheids is not alarming, and  $[\text{Fe}/\text{H}]$  is indistinguishable. In terms of age, QZ Nor seems to be slightly older than V340 Nor ( $7.85 \pm 0.07$  vs.  $7.60 \pm 0.08$ ), and better matches to the cluster's age ( $8.08 \pm 0.23$ , D02).

In summary, the two Cepheids have differing parallax and age. The cluster values from D02 happen to lie between the two, oddly enough favoring QZ Nor, which lies at greater separation from the cluster's core. Therefore, the cluster parameters may require reconsideration. Since NGC 6067 is located in the Norma cloud (cf. atlas page in K05), the determination of cluster radii is rather difficult. Differential reddening may be important to resolve this conundrum (higher for V340 Nor which is closer to cluster center). We therefore note that there are some issues with the membership constraints employed here, and detailed follow-up of the cluster is required. Until then, the constraints compiled are consistent with membership for both Cepheids, and we consider both to be *bona fide* cluster members.

**4.1.2.2 CV Mon and vanden Bergh 1** CV Mon lies right in the center of cluster van den Bergh 1 and was studied in detail by Turner et al. (1998). The constraints employed are parallax, radial velocity, proper motion, and age, and yield a likelihood of 32%, which is low due to the discrepant  $\mu_\alpha^*$ . The average cluster RV determined by Rastorguev et al. (1999) is identical to that of CV Mon and no information on the number of stars involved in its determination is given; it should thus be discarded as membership constraint (this would lower the likelihood to 20%). Aside from this, the cluster data from D02 is largely consistent with the data for the Cepheid. Parallax (also reddening),  $\mu_\delta$ , and age agree well between cluster and Cepheid. Thus, the Cepheid likely lies inside the volume occupied by the Cluster, and therefore should be considered to be a *bona fide* CC. Observational

**Table 1.** Results of our membership analysis for combinations known in the literature. Constraints indicated are parallax,  $\varpi$ , radial velocity,  $v_r$ , proper motion,  $\mu_\alpha^*$  and  $\mu_\delta$ , iron abundance [Fe/H], and age. Filled circles indicate constraints consistent between Cepheid and cluster, greater deviations are stated explicitly in units of the square-summed uncertainties. Open circles indicate unavailable membership constraints.  $R_{\text{Cl}}$  denotes the distance in parsecs of the Cepheid from cluster center, assuming membership and the cluster’s heliocentric distance.  $P(A)$  is the prior used, asterisks mark  $P(A)$  values based on D02 apparent diameters. Column  $P(B|A)$  lists likelihoods, and  $P(A|B)$  the combined membership probability. The last column CC indicates qualitatively, how membership is judged for a particular Combo: ‘y’ denotes *bona fide* CCs; ‘i’ denotes that the data available yield an inconclusive result; ‘u’ denotes unlikely membership; ‘n’ denotes Combos that are clearly inconsistent with membership. Column Ref. lists some pertinent references: a: Irwin (1955), b: Kholopov (1956), c: Feast (1957), d: Sandage (1958), e: Eggen (1980), f: Turner (1982), g: Walker (1985b), h: Turner (1986), i: Turner et al. (1992), j: Matthews et al. (1995), k: Turner et al. (1997), l: Hoyle et al. (2003), m: An et al. (2007), n: Turner (2010), o: Turner (1981), p: Flower (1978), q: Walker (1985a), r: Turner et al. (1998), s: Turner & Pedreros (1985), t: Turner (1980), u: Yilmaz (1966), v: Turner (1998), w: Turner & Burke (2002), x: Turner (1976), y: Walker (1987), z: Turner et al. (1994), A: Turner et al. (1993), B: Turner (1992), C: Majaess et al. (2011), D: Vazquez & Feinstein (1990), E: Baumgardt et al. (2000), F: Turner et al. (2008), G: Balona & Laney (1995), H: Turner (1977)

Cluster	Cepheid	Constraints						$R_{\text{cl}}$ [pc]	$P(A)$	$P(B A)$	$P(A B)$	CC	Ref.
		$\varpi$	$v_r$	$\mu_\alpha^*$	$\mu_\delta$	[Fe/H]	age						
IC 4725	U Sgr	•	•	•	•	•	•	0.3	1.0	0.984	0.984	y	abcm
NGC 7790	CF Cas	•	•	•	•	•	•	0.9	0.955	0.975	0.931	y	dj
NGC 129	DL Cas	•	•	•	•	•	•	0.2	1.0	0.857	0.857	y	bi
Turner 9	SU Cyg	•	•	•	•	•	1.2 $\sigma$	0.0	1.0	0.807	0.807	y	kn
NGC 7790	CE Cas A	•	•	•	•	•	•	1.5	0.71	0.975	0.693	y	dj
NGC 7790	CE Cas B	•	•	•	•	•	•	1.6	0.697	0.956	0.666	y	dj
NGC 6649	V367 Sct	•	•	•	1.3 $\sigma$	•	•	1.0	0.884*	0.65	0.574	y	op
NGC 6067	V340 Nor	•	•	•	•	•	1.9 $\sigma$	0.6	1.0	0.573	0.573	y	gmnl
Lyngå 6	TW Nor	1.2 $\sigma$	•	•	1.3 $\sigma$	•	•	0.6	1.0*	0.453	0.453	y	nmqC
vdBergh 1	CV Mon	•	•	2.2 $\sigma$	•	•	•	0.6	1.0	0.318	0.318	y	r
NGC 6087	S Nor	•	•	1.2 $\sigma$	2.0 $\sigma$	1.2 $\sigma$	1.3 $\sigma$	0.6	1.0	0.192	0.192	y	abch
Trumpler 35	RU Sct	1.3 $\sigma$	•	•	•	•	•	5.1	0.194*	0.840	0.163	y	nltu
Collinder 394	BB Sgr	1.0 $\sigma$	•	•	1.2 $\sigma$	•	•	3.7	0.208	0.637	0.133	y	ns
Turner 2	WZ Sgr	•	•	•	2.2 $\sigma$	•	•	5.3	0.337*	0.287	0.097	y	A
Trumpler 18	GH Car	•	1.4 $\sigma$	•	•	•	2.0 $\sigma$	2.9	0.194	0.143	0.028	u	DE
NGC 6067	QZ Nor	•	•	•	•	•	•	7.4	0.029	0.963	0.027	y	eg
Berkeley 58	CG Cas	•	•	•	3.3 $\sigma$	•	•	5.0	0.308	0.027	0.008	y	F
NGC 5662	V Cen	•	•	•	•	•	•	5.8	0.006	0.958	0.006	y	fmn
NGC 6664	EV Sct	•	•	•	•	•	•	7.5	0.0	0.866	0.0	y	wx
Ruprecht 173	X Cyg	•	•	•	•	•	•	—	0.878*	1.0	0.878	i	nvw
Dolidze 45	V1334 Cyg	•	•	•	•	•	•	—	0.017*	1.0	0.017	i	n
Ruprecht 79	CS Vel	1.8 $\sigma$	1.5 $\sigma$	1.2 $\sigma$	1.9 $\sigma$	•	2.3 $\sigma$	1.5	1.0	0.007	0.007	i	ny
Platais 1	V1726 Cyg	•	3.2 $\sigma$	•	1.0 $\sigma$	•	1.8 $\sigma$	1.4	0.98	0.006	0.006	i	z
NGC 1647	SZ Tau	•	1.8 $\sigma$	•	2.6 $\sigma$	•	1.2 $\sigma$	20.1	0.0	0.047	0.0	u	B
NGC 3496	V442 Car	•	•	1.1 $\sigma$	2.3 $\sigma$	•	•	1.0	0.625	0.039	0.024	n	G
King 4	UY Per	1.3 $\sigma$	•	1.6 $\sigma$	2.6 $\sigma$	•	•	12.6	0.021	0.019	0.0	n	H
Turner 5	T Ant	4.3 $\sigma$	•	3.3 $\sigma$	4.5 $\sigma$	•	3.2 $\sigma$	0.0	1.0	0.0	0.0	n	w
NGC 4349	R Cru	6.8 $\sigma$	•	2.1 $\sigma$	1.1 $\sigma$	2.1 $\sigma$	2.3 $\sigma$	9.5	0.048	0.0	0.0	n	w
NGC 4349	T Cru	6.7 $\sigma$	•	2.1 $\sigma$	•	2.2 $\sigma$	2.5 $\sigma$	19.9	0.0	0.0	0.0	n	w
NGC 2345	TV CMa	•	5.6 $\sigma$	•	•	•	•	25.0	0.001	0.0	0.0	n	xw

follow-up of cluster proper motion and radial velocity would be beneficial.

**4.1.2.3 S Nor and NGC 6087** S Nor’s membership in NGC 6087 was among the first to ever be suggested (Irwin 1955) and confirmed using radial velocities (Feast 1957), as well as the detailed study by Turner (1986) based on reddening and distance.

The values for the cluster’s mean RV differ greatly between D02 (6 km s<sup>−1</sup>), K05 (−9 km s<sup>−1</sup>), and Feast (1957, 2.0 km s<sup>−1</sup>), which is important considering the Cepheid’s  $v_\gamma = 2.53$  km s<sup>−1</sup> (Groenewegen 2008). We note that the value adopted by D02 is measured on the Cepheid itself (Mermilliod et al. 2008), although without taking orbital motion into account, and is therefore not suitable as a

membership constraint. Since Feast (1957) investigated the largest number of stars and specifically targeted this cluster, we trust that their 2.0 km s<sup>−1</sup> is the best available estimate for the mean velocity of the cluster.

We note that proper motion, reddening, metallicity, and age are slightly discrepant between cluster and Cepheid, resulting in a low likelihood. However, these differences barely exceed the combined uncertainties and may not be significant.

**4.1.2.4 RU Sct and Trumpler 35** Based on age and distance from D02, this Combo would appear nearly inconsistent with membership. Unfortunately, the average cluster RV appears to have been measured on the Cepheid (Rastorguev et al. 1999) and can therefore not be consid-

ered a valid membership constraint. Membership of RU Sct in Trumpler 35 was studied in detail by Turner (1980), Hoyle et al. (2003), and T10. Closer inspection of these references reveals an underestimated cluster distance in D02 (compared also to Yilmaz 1966). The region around the Cepheid contains multiple associations, which may explain the confusion in D02. Using the cluster parallax and age from Turner (1980), we compute a likelihood of 84 %, and consider RU Sct a *bona fide* member of Trumpler 35.

**4.1.2.5 BB Sgr and Collinder 394** BB Sgr lies at 21' separation from Collinder 394's center, i.e., at a distance of 3.7 pc assuming membership. This Combo was first studied in detail by Turner & Pedreros (1985) after having been originally suggested by Tsarevsky et al. (1966). Most membership constraints could be employed and there are only small discrepancies in parallax and  $\mu_s$ . The low prior may be misleading in this case, since the high likelihood indicates membership. We thus consider BB Sgr a *bona fide* member of Collinder 394.

**4.1.2.6 WZ Sgr and Turner 2** This Combo was first discussed by Turner et al. (1993) when the cluster was first discovered. Most membership constraints compiled from D02, i.e., parallax,  $\mu_s$ , and age, differ between Cepheid and cluster, which would result in a likelihood of  $< 1\%$ . The cluster parameters listed in D02 were taken from the automated, 2MASS-based study by Tadross (2008). However, the much more detailed study by Turner et al. (1993) should be given higher weight, especially for its thorough treatment of reddening, and the more precise photometry used. Hence, we compute the likelihood using the cluster parameters for parallax and age from Turner et al. (1993) and find a combined membership probability of 10 %. The sole discrepant membership constraint remains proper motion. However, this discrepancy alone is not sufficiently strong to indicate non-membership.

**4.1.2.7 CG Cas - Berkeley 58** CG Cas lies at a separation of 5.7' (outside  $r_c$ ) from Berkeley 58's center, at roughly half the limiting radius. While the Cepheid's PLR-based parallax is close to that of the cluster and reddening is in agreement,  $\mu_s$  is discrepant by  $3.3\sigma$  and does not suggest a common point of origin. However, Turner et al. (2008) conclude in favor of membership based on a detailed study involving age, reddening, distance and radial velocity. Since the cluster is located in the Perseus spiral arm, the proper motion estimate in K12 may well be dominated by Galactic motion. Hence, the likelihood computed here is likely underestimated, and we should trust the result by Turner et al. (2008).

**4.1.2.8 V Cen and NGC 5662** Despite the low prior, all membership constraints indicate V Cen's membership in NGC 5662, yielding a very high likelihood of 92 %. At NGC 5662's distance of 666 pc, the Cepheid lies 5.8 pc from cluster center. Hence, the prior may be misleading in this

case, perhaps due to underestimated radii. We therefore consider V Cen a *bona fide* CC of NGC 5662<sup>13</sup>.

**4.1.2.9 EV Sct and NGC 6664** This Combo, mentioned previously in Turner (1976) and Turner & Burke (2002), would be nearly inconsistent with membership if the cluster values listed in D02 are employed in the calculation: the highly discrepant age ( $2.5\sigma$ ) and parallax ( $0.57 \pm 0.09$  vs.  $0.86 \pm 0.17$ ) would result in a likelihood of 13 %. However, a literature study reveals that the distance and age listed in D02 may be wrong. The distance by (Arp 1958) and Schmidt (1982) are both much greater than the 1.1 kpc in D02. We thus adopt the distance and age by (Schmidt 1982, 1.4 kpc) and obtain a very high likelihood of 87 %, using also proper motion and radial velocity. As already noted by Laney & Caldwell (2007), a modern follow-up campaign is warranted for this cluster.

## 4.2 New Combos of Interest

Our results suggest the following new *bona fide* CCs: SX Car in ASCC 61, ASAS J182714-1507.1 in Kharchenko 3, S Mus in ASCC 69, UW Car in Collinder 220, and V379 Cas in NGC 129, see Tab. 2. We discuss these Combos in some detail in the paragraphs below, followed by the identification of some unconstrained high-prior Combos recovered by our work. Some Combos flagged as inconclusive or unlikely members are discussed in appendix A.

### 4.2.1 New candidate CCs

**4.2.1.1 SX Car and ASCC 61** The 4.86 d Cepheid SX Car is seen to be co-moving with ASCC 61 in proper motion. Unfortunately, no average cluster RV is known. Parallax and age, however, agree very well between cluster and Cepheid, lending support to the hypothesis of membership with  $P(B|A) = 92\%$ . An in-depth analysis of the cluster, including its mean RV, is of the essence, since the cluster is located in a crowded field (K05). We tentatively consider SX Car as a member of ASCC 61.

### 4.2.1.2 ASAS J182714-1507.1 and Kharchenko 3

The 5.5 d fundamental-mode pulsator ASAS J182714-1507.1 = TYC 6266-797-1 lies at a large separation of 71' from cluster center, which translates to approximately 44 pc at the cluster's estimated heliocentric distance of 2.1 kpc and casts some doubt on possible membership.

Reddening for cluster and Cepheid (estimated from 2MASS photometry, see Sec. 3.2.1.2) are in excellent agreement, while parallax and age are also consistent with membership. Proper motion does not exceed its error bars and it thus of limited constraining power in this case. Detailed observational follow-up is warranted for both Cepheid and cluster.

<sup>13</sup> According to Turner (2013, priv. comm.), NGC 5662 is actually a double cluster, and V Cen belongs to NGC 5662b.



**Table 2.** New Combos of interest. Columns are described in Tab.1. We visually separate a) Combos with membership constraints that lie inside the core of a cluster, b) Combos with high likelihood for which  $\varpi$  was available, c) Combos without  $\varpi$  that yield high likelihoods, and d) Combos for which no likelihoods could be computed, but that lie close to the core of their potential host clusters. Combos judged unlikely (‘u’) or bona-fide (‘y’) are discussed separately in the text. Inconclusive Combos (‘i’) require additional data or stronger membership constraints.

Cluster	Cepheid	Constraints						$R_{cl}$ [pc]	$P(A)$	$P(B A)$	$P(A B)$	CC
		$\varpi$	$v_r$	$\mu_\alpha^*$	$\mu_\delta$	[Fe/H]	age					
ASCC 60	Y Car	○	●	●	●	○	○	0.3	1.0	0.786	0.786	i
ASCC 61	SX Car	●	○	●	●	○	●	20.4	0.001	0.919	0.001	y
Kharchenko 3	ASAS J182714-1507.1	●	○	●	●	○	●	43.9	0.004*	0.905	0.004	y
ASCC 69	S Mus	●	●	●	●	○	1.0 $\sigma$	11.4	0.004	0.879	0.004	y
Collinder 220	UW Car	●	●	●	●	○	1.1 $\sigma$	47.2	0.001*	0.838	0.001	y
IC 4725	Y Sgr	1.2 $\sigma$	●	●	●	●	●	26.8	0.0	0.781	0.0	u
NGC 6705	ASAS J184741-0654.4	●	●	1.3 $\sigma$	●	○	○	34.6	0.0	0.778	0.0	i
King 4	GO Cas	●	○	●	●	○	1.3 $\sigma$	21.7	0.0	0.684	0.0	i
Berkeley 60	BF Cas	●	○	●	●	○	1.1 $\sigma$	33.9	0.0	0.672	0.0	i
Toepler 1	GI Cyg	1.0 $\sigma$	○	○	○	○	●	18.7	0.0	0.568	0.0	i
Feinstein 1	U Car	●	1.6 $\sigma$	●	●	○	●	20.8	0.0	0.52	0.0	i
ASCC 61	VY Car	●	○	●	●	○	2.0 $\sigma$	21.9	0.0	0.385	0.0	i
NGC 129	V379 Cas	○	●	●	●	○	●	20.3	0.0	0.896	0.0	y
Ruprecht 18	VZ CMa	○	○	●	1.2 $\sigma$	●	●	9.2	0.0	0.592	0.0	i
Berkeley 82	ASAS J190929+1232.8	○	○	●	●	○	1.3 $\sigma$	10.9	0.0*	0.549	0.0	i
Ruprecht 118	ASAS J162811-5111.9	○	○	●	1.1 $\sigma$	○	●	22.2	0.0*	0.536	0.0	i
Hogg 12	GH Car	○	○	●	1.1 $\sigma$	○	1.1 $\sigma$	9.8	0.0	0.503	0.0	i
NGC 6649	ASAS J183652-0907.1	○	●	●	1.1 $\sigma$	○	1.3 $\sigma$	36.7	0.0*	0.469	0.0	i
Trumpler 9	ASAS J075503-2614.3	○	○	1.1 $\sigma$	1.1 $\sigma$	○	●	15.2	0.0	0.463	0.0	i
NGC 2345	ASAS J070911-1217.2	○	○	●	1.8 $\sigma$	○	●	36.6	0.0	0.317	0.0	i
Ruprecht 100	NSV 19202	○	○	○	○	○	○	–	0.837*	1.0	0.837	i
FSR 1595	NSV 18905	○	○	○	○	○	○	–	0.821*	1.0	0.821	i
Dolidze 53	V415 Vul	○	○	○	○	○	○	–	0.759*	1.0	0.759	i
Ruprecht 100	TY Cru	○	○	○	○	○	○	–	0.671*	1.0	0.671	i
SAI 116	NSV 18942	○	○	○	○	○	○	3.4	0.621*	1.0	0.621	i
Dolidze 34	TY Sct	○	○	○	○	○	○	–	0.547	1.0	0.547	i

**4.2.1.3 S Mus and ASCC 69** The membership constraints considered (all but [Fe/H]) for the binary Cepheid S Mus (e.g. Petterson et al. 2005) and ASCC 69 yield a very high likelihood of 88 %. ASCC 69 is a sparsely populated cluster for which K05 list merely twelve 1- $\sigma$  members. Cluster radius and center coordinates may therefore be rather imprecise. Furthermore, radial velocities are only of limited value as membership constraints, since the average cluster RV is based on only 2 stars. However, proper motion clearly indicates that cluster and Cepheid are co-moving. We tentatively accept S Mus as a cluster member and stress the need for a detailed study of its candidate host cluster ASCC 69.

**4.2.1.4 UW Car and Collinder 220** This new Combo yields a likelihood of 84 % from all membership constraints but [Fe/H]. The parallax of the Cepheid is estimated by the PLR, cf. Sec. 3.1.2. The most compelling evidence of membership comes from proper motion, while the large on-sky separation translates into a distance of 47 pc from cluster center assuming the cluster’s distance. A detailed review of the cluster’s parameters, as well as a better parallax estimate of the Cepheid would help to conclude on this Combo.

**4.2.1.5 V379 Cas and NGC 129** This high likelihood pair at large separation (44’ or 20 pc at the estimated distance to NGC 129) has nearly vanishing proper motion,

while the both RVs are in excellent agreement and the ages are consistent. We obtain a likelihood of 91 %. No parallax is computed, since V379 Cas is an overtone pulsator. Since NGC 129 has another known member, DL Cas, we can compare the pulsational ages of the two Cepheids and find both to be consistent within the uncertainties ( $7.70 \pm 0.08$  for DL Cas and  $7.83 \pm 0.07$  for V379 Cas). Furthermore, the iron abundances of both Cepheids are close, as are their RVs (to within less than  $1 \text{ km s}^{-1}$ ). We further note that V379 Cas and DL Cas have similar reddening values, though  $E(B - V)$  of V379 Cas is slightly (0.1 mag) higher (Kovtyukh et al. 2008, both). We therefore tentatively consider V379 Cas a member of NGC 129’s Halo, pending a better distance estimate and additional membership constraints. NGC 129 is thus particularly interesting, containing both a fundamental-mode and an overtone pulsator, just as NGC 6067.

#### 4.2.2 Unconstrained High-prior Combos

In Tab. 2, we highlight six Combos with  $P(A) > 50\%$  that have thus far not been studied for membership, and for which no membership constraints were available. Hence, no likelihoods could be computed for these cases. We therefore suggest the following Combos for observational follow-up: V415 Vul – Dolidze 53; TY Cru & NSV 19202 –

Ruprecht 100; NSV 18942 – SAI 116; TY Sct – Dolidze 34; NSV 18905 – FSR 1595.

### 4.3 The Galactic Cepheid PLR revisited

Let us now employ our *bona-fide* CC sample to revisit the calibration of the Galactic Cepheid period-luminosity relationship. It represents an ideal sample to this end, due to the high confidence we can have in cluster membership, though small statistics and a lack of long-period calibrators will limit the precision attainable.

A Cepheid’s absolute V-band magnitude,  $M_V$ , is determined using the true distance modulus of the cluster,  $(V_0 - M_V)_{\text{Cl}}$ , the Cepheid’s mean magnitude,  $\langle m_V \rangle$ , the ratio of total-to-selective extinction towards the cluster,  $R_{V,\text{Cl}}$ , and the Cepheid’s color excess,  $E(B - V)$ , as

$$M_V = \langle m_V \rangle - (V_0 - M_V)_{\text{Cl}} - R_{V,\text{Cl}}E(B - V), \quad (18)$$

where quantities refer to the Cepheid, unless subscripted by ‘Cl’.

As described in Sec. 3.1, we compile cluster data from D02 for our membership analysis. These data, however, do not take into account line-of-sight dependencies of reddening, or non-canonical values of  $R_V$ . In the following, we refer to the set of data compiled for our membership analysis as the ‘standard’ set.

In an attempt to improve accuracy, we compile more accurate data from detailed studies of the host clusters. True distance moduli based on ZAMS-fitting were taken from T10 and An et al. (2007), giving preference to the estimates with the smallest uncertainties. For the two ASCC clusters, we use the de-reddened values by Kharchenko et al. (2005a), and for Collinder 220 we rely on the data in D02. For reddening, An et al. (2007) provide a convenient way to calculate  $R_V$  for some lines of sight in our sample as  $R_V = R_{V,0} + 0.22(B - V)_0$ , with  $R_{V,0}$  tabulated for the cluster and taking into account the intrinsic color of the Cepheids. For the two ASCC clusters and Collinder 220, we employ the canonical  $R_V = 3.1 \pm 0.2$  since no other estimate is available. For Turner 9, Berkeley 58, and van den Bergh 1, we use the distance moduli and  $R_V$  values from Turner et al. (1997, 2008, 1998), respectively. For the long period Cepheid hosts, Trumpler 35 and Turner 2, we employ the data published in Turner (1980) and Turner et al. (1993). Cepheid mean V-magnitudes and  $E(B - V)$  were compiled as described in Sec. 3.1. Note that ASAS J182714 – 1507.1 was not included in this calibration, since the data compiled were not of sufficient quality. The values thus compiled are listed in Tab. 3, and we refer to this data set as the ‘optimal’ one.

Figure 17 shows the fits to both the ‘standard’ (left panel) and the ‘optimal’ (right panel) data sets. In both figures, four straight lines indicate the PLR calibrations by Tammann et al. (2003, red dash-dotted), Turner et al. (2010, green dotted, lower zero-point), as well as our non-weighted (dashed cyan), and weighted (solid blue) least-squares fits to the data. The large scatter (RMS=0.61) in the ‘standard’ data set is striking. Contrastingly, the ‘optimal’ set is much better indeed, with an RMS of 0.24 mag. Hence, it is evident that the cluster data compiled for the membership analysis is rather limited in precision and sometimes also accuracy, a fact we already encountered when computing membership probabilities, see for instance the case of

WZ Sgr in Sec. 4.1.2.6. Thus, there remains a need for detailed and deep photometric studies of open cluster parameters, and in particular reddening.

We determine the uncertainties on the ‘optimal’ set by linear regression and obtain:

$$\langle M_V \rangle = -(2.88 \pm 0.18) \log P - (1.02 \pm 0.16). \quad (19)$$

Despite the reasonable formal uncertainties of our ‘optimal’ fit, our solution should not be considered definitive. The result of the fit is very sensitive to the absolute magnitude estimates of the extreme points at short and long periods, and the  $M_V$  estimates of the new candidates are clearly too crude at this point. Furthermore, despite our preference for cluster literature with the smallest uncertainties, there is no guarantee that the most accurate cluster data was employed; there appears to exist too little consensus on some clusters in the literature, e.g. for Lyngå 6,  $(V_0 - M_V)_{\text{Cl}}$  differs by 0.39 mag between T10 and An et al. (2007), exceeding the published combined uncertainties by a factor greater than 3. Binarity of the Cepheids was not accounted for, since the fit is dominated mainly by the cluster parameters. Yet, we note that our result is consistent with the calibration by T10 ( $\langle M_V \rangle = -(2.78 \pm 0.12) \log P - (1.29 \pm 0.10)$ ), which is to be expected due to the significant overlap in the sample of CCs used for this calibration.

## 5 DISCUSSION

### 5.1 Constraining Power and Limitations of Membership Constraints

#### 5.1.1 The Prior $P(A)$

The form of the prior was motivated by radial density profiles of star clusters, see Sec. 2.1. However, the degree with which the distribution of stars in the cluster is known varies greatly between clusters, and deviations from circular cluster shapes were ignored for internal consistency. Furthermore, crowding, great distances ( $\sim$  kpc) to host cluster candidates, differential reddening, sparsity, etc. all conspire to complicate the definition of cluster radii. It is thus not surprising that the prior does not perform extremely well as a membership constraint if taken at face value. Nevertheless, it does help to separate the interesting cases from the majority of null matches, since it reduces the question of proximity on the projected sky to a single number that contains information on the density of the cluster, since both cluster radii are used in its definition.

**5.1.1.1 Chance Alignment** Among our (*bona fide* or inconclusive) CCs, 7–9 are found to lie within  $r_c$ , and 8–17 at  $r_c < R < r_{\text{lim}}$ . Within the original cross-match, 25 Combs are matched within  $r_c$  and 520 within  $r_c < R < r_{\text{lim}}$ . Thus we can estimate the rate of chance alignment within the core radius to be approximately 3 : 1. At separations inferior to  $r_{\text{lim}}$ , this ratio increases to between 20 : 1 and 35 : 1, depending on whether inconclusive cases are counted, or not.

Note that 8 *bona-fide* CCs lie outside  $r_{\text{lim}}$ , 6 of which are located within two  $r_{\text{lim}}$ ; EV Scuti’s separation from NGC 6664’s center is  $2.6 r_{\text{lim}}$ , and that of V379 Cas from NGC 129 is  $2.7 r_{\text{lim}}$ .

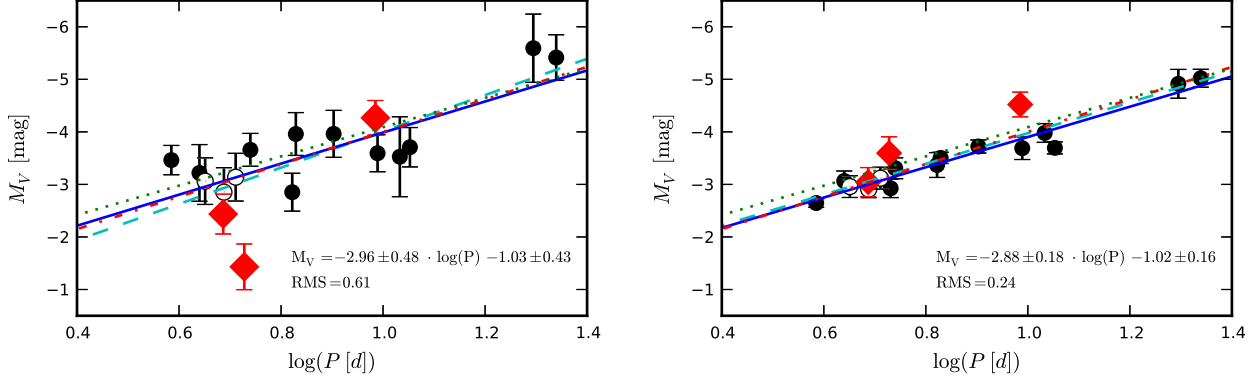


**Figure 17.** Cepheid PLRs fitted to the ‘standard’ (left panel) and ‘optimal’ (right panel) data sets. Solid circles indicate previously known CCs, open circles highlight the three Cepheids in NGC 7790. Solid red large diamonds indicate the new *bona-fide* fundamental-mode CCs S Mus, SX Car, and UW Car included in the fit. The dotted line shows the PLR by Benedict et al. 2007, and the dash-dotted line represents Tammann et al. (2003). Solid and dashed lines indicate weighted and non-weighted least-squares fits. An accurate PLR calibration critically depends on accurate distance estimates from detailed studies that include line-of-sight-variations of extinction.

Cepheid	Cluster	$\langle m_V \rangle$	$E(B - V)$	$(V_0 - M_V)$	$R_{V,Cl}$	$\log P$	$M_V$
SU Cyg	Turner 9	6.89	$0.07 \pm 0.02$	$9.33 \pm 0.05$	$2.94 \pm 0.38$	0.585	$-2.65 \pm 0.08$
CG Cas	Berkeley 58	11.37	$0.69 \pm 0.01$	$12.40 \pm 0.12$	$2.95 \pm 0.20$	0.640	$-3.07 \pm 0.19$
CE Cas B	NGC 7790	11.09	$0.48 \pm 0.05$	$12.46 \pm 0.01$	$3.31 \pm 0.26$	0.651	$-2.98 \pm 0.21$
SX Car*	ASCC 61	9.12	$0.33 \pm 0.03$	$11.14 \pm 0.20$	$3.10 \pm 0.51$	0.687	$-3.04 \pm 0.28$
CF Cas	NGC 7790	11.15	$0.48 \pm 0.03$	$12.46 \pm 0.01$	$3.33 \pm 0.26$	0.688	$-2.91 \pm 0.16$
CE Cas A	NGC 7790	10.94	$0.48 \pm 0.05$	$12.46 \pm 0.01$	$3.33 \pm 0.26$	0.711	$-3.12 \pm 0.21$
UW Car*	Collinder 220	9.46	$0.46 \pm 0.01$	$11.63 \pm 0.20$	$3.10 \pm 0.51$	0.728	$-3.60 \pm 0.31$
CV Mon	vdBergh 1	10.33	$0.68 \pm 0.05$	$11.08 \pm 0.07$	$3.20 \pm 0.04$	0.731	$-2.93 \pm 0.18$
V Cen	NGC 5662	6.87	$0.25 \pm 0.05$	$9.31 \pm 0.02$	$3.47 \pm 0.38$	0.740	$-3.32 \pm 0.20$
BB Sgr	Collinder 394	6.91	$0.29 \pm 0.05$	$9.38 \pm 0.10$	$3.10 \pm 0.51$	0.822	$-3.37 \pm 0.24$
U Sgr	IC 4725	6.72	$0.39 \pm 0.02$	$8.93 \pm 0.02$	$3.32 \pm 0.21$	0.829	$-3.52 \pm 0.11$
DL Cas	NGC 129	8.98	$0.46 \pm 0.02$	$11.11 \pm 0.02$	$3.46 \pm 0.22$	0.903	$-3.73 \pm 0.13$
S Mus*	ASCC 69	6.13	$0.21 \pm 0.02$	$10.0 \pm 0.20$	$3.10 \pm 0.51$	0.985	$-4.52 \pm 0.24$
S Nor	NGC 6087	6.41	$0.12 \pm 0.05$	$9.65 \pm 0.03$	$3.74 \pm 0.85$	0.989	$-3.70 \pm 0.22$
TW Nor	Lynga 6	11.66	$1.24 \pm 0.03$	$11.51 \pm 0.08$	$3.33 \pm 0.10$	1.033	$-3.96 \pm 0.18$
V340 Nor	NGC 6067	8.41	$0.32 \pm 0.02$	$11.03 \pm 0.01$	$3.36 \pm 0.29$	1.053	$-3.68 \pm 0.11$
RU Sct	Trumpler 35	9.53	$0.92 \pm 0.03$	$11.58 \pm 0.18$	$3.10 \pm 0.20$	1.295	$-4.91 \pm 0.27$
WZ Sgr	Turner 2	8.09	$0.62 \pm 0.02$	$11.26 \pm 0.10$	$3.00 \pm 0.20$	1.339	$-5.02 \pm 0.17$

**Table 3.** Parameters adopted for the ‘optimal’ set used in Eq. 18 and the right panel of Fig. 17. Newly-identified *bona fide* Combos employed in the fit are marked with an asterisk next to the Cepheids identifier. True distance moduli of clusters,  $(V_0 - M_V)$ , and absorption-relevant parameters were adopted according to the criteria specified in the text. We adopt 0.04 mag as the uncertainty on  $\langle m_V \rangle$ .

### 5.1.2 The Likelihood $P(B|A)$

Intuitively, the greatest set of constraints used provides the tightest constraints on membership for any cluster-Cepheid combination (Combo). Figure 18 illustrates this. It shows a logarithmic normalized histogram of likelihoods for two cases: more than 3 constraints used to calculate  $P(B|A)$  (light gray distribution); all constraints used to calculate  $P(B|A)$  (dark gray slim bars). However, the constraining power of a given set of constraints is not merely a function of its size. Here we discuss the membership constraining power of the different constraints used to calculate likelihoods.

**Proper motions** can be very effective at ruling out membership if the motion clearly exceeds the uncertainties on the measurement. This is the case for a cluster cross-matched with a background Cepheid, for instance. However, for a significant fraction of Combos, the proper motion vec-

tor’s magnitude was smaller than the uncertainty of the measurement, thus effectively not constraining membership, see Fig 19. If the magnitude surpasses the uncertainties by at least a factor of 3, proper motion serves as a reliable constraint. For the majority of Combos that fulfill this criterion, membership tends to be excluded.

**Distance** is a potentially very strong membership constraint, since intuitively, a Cepheid that occupies the same space volume as a cluster should be a member. However, cluster distances can be subject to large systematic uncertainties due to parameter degeneracy (distance, age, reddening), model-dependence (rotation, etc.), or previous distance estimates to, e.g., the Pleiades. Furthermore, implicit assumptions on cluster membership can significantly impact the distance determined, especially for relatively young clusters that harbor few stars around the Main-sequence turn-

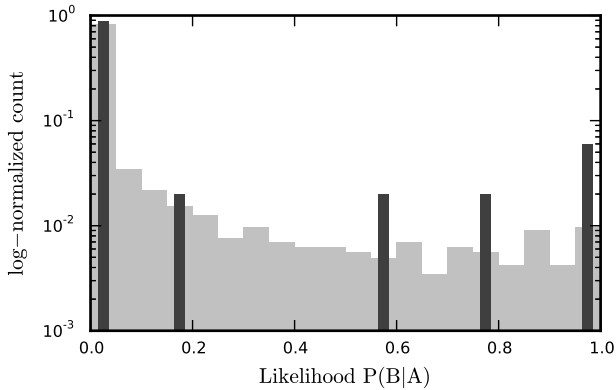


**Figure 18.** Log-normalized histogram of likelihoods. Light gray, broad bars: Combinations with 3 or more parameters used for  $P(B|A)$ . Dark gray, slim bars: Combinations with all membership constraints. The more membership constraints are employed, the more separated are high and low likelihoods, i.e. the better constraint is membership.

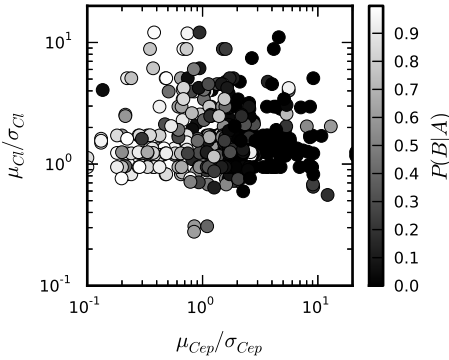


**Figure 19.** Likelihoods computed as a function of proper motion. Abscissa: proper motion of Cepheid divided by the squared-summed uncertainties, i.e.  $\mu = \sqrt{(\mu_\alpha^*)^2 + \mu_\delta^2}$ ;  $\sigma = \sqrt{\sigma(\mu_\alpha^*)^2 + \sigma(\mu_\delta)^2}$ . Ordinate: same for Cluster.

off and few or no red giants. Very detailed studies of open clusters, and in particular of the line-of-sight extinction, are required for improvement in this domain, as is shown in Sec. 4.3, or demonstrated by the discussion of CV Mon’s membership in van den Bergh 1 (cf. Sec. 4.1.2.2).

**Radial velocities** have the potential to provide very tight membership constraints, since the RV dispersion within open clusters can be significantly below  $1 \text{ km s}^{-1}$  (Lovis & Mayor 2007), approaching the measurement precision on  $v_\gamma$  for non-binary Cepheids. However, estimates of average cluster RVs are usually based on only a few stars, see Fig. 6. In fact, approximately half of all clusters with ‘known’ average RVs are based on measurements of two stars or less, and strong selection effects (e.g. toward late-type stars) can severely impact the estimate. Since Cepheids are very bright and of late spectral type, it is rather likely that a cluster RV is in part based on measurements that include a Cepheid. We therefore highlight the need to observe more radial velocities of upper main sequence stars in clusters in order to ensure the most accurate estimates of average cluster RV. Alterna-

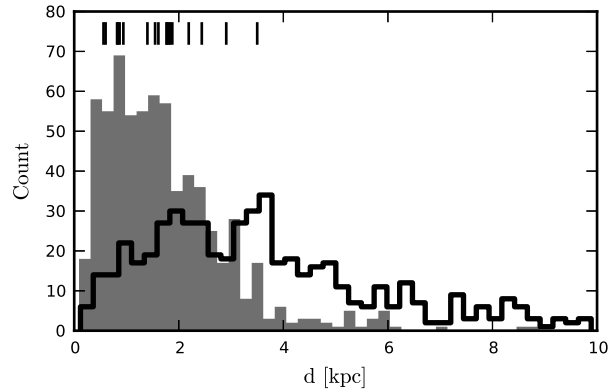


**Figure 20.** Distance distribution of known open clusters in log-age range [7.0, 8.5] (gray filled histogram, high peak at small  $d$ ) and of Cepheids at low Galactic latitudes,  $|b| \leq 10^\circ$  (black step histogram). Distances of *bona-fide* CCs from this work indicated by short black lines at the top.

tively, larger telescopes may observe the much fainter lower main sequence. The Gaia-ESO public spectroscopic survey Gilmore et al. (2012) will soon provide precise RVs for a large number of clusters and thus can improve the reliability of a future study similar to the present one.

The **iron abundances** compiled here were, arguably, of limited use as membership constraints, since data inhomogeneity, the limited number of cluster stars used for determining the cluster average, and differences in the solar reference values used are at the same order of magnitude as the range of iron abundances found in the sample considered (that lies within the young metal-rich Galactic disk). For a few cases, however, the iron abundance did further strengthen the interpretation of excluded membership.

**Age** as a membership constraint quantifies valid evolutionary considerations that are established empirically. It is a particularly useful membership constraint, since it is readily available for clusters as well as for Cepheids (from period-age relations), especially when few other constraints are available. However, ages for both kinds of objects are subject to model-dependence, and the accuracy of the values inferred is difficult to quantify.

All of the above quantities have their own peculiarities, and thus no single one can be named the ‘best’ membership constraint. Instead, the greatest constraining power resides in the combination of all the data, as is seen in the *bona-fide* CCs identified in this work, as well as in Fig. 18.

### 5.1.3 Membership Probabilities $P(A|B)$

We computed  $P(A|B)$  simply as the product of the prior and the likelihood, leaving out the normalization term  $P(B)$  that would in principle be required, see Eq. 1. However, in order to make full use of the  $P(A|B)$  values computed,  $P(B)$  should not be neglected. Given that the incompleteness for open clusters is quite significant at heliocentric distances greater than, say, 1 kpc, we did not currently see this as feasible, cf. Fig. 20.

## 5.2 Incompleteness

Despite our aim to maximize the number of clusters and Cepheids considered, only 23 *bona fide* CCs were identified. This is a result of the apparent difference in sample completeness for clusters and Cepheids. Fig. 20 shows the histograms of heliocentric open cluster distances for clusters with the appropriate age range ( $\log_{10}(\text{age}[\text{yr}]) = [7.0, 8.5]$ ), taken from D02 as the grey filled distribution (peak at smaller  $d$ ), and the Cepheid distances compiled (cf. Sec. 3.2.1, black step histogram). It is evident that the detection rate of open clusters stalls at distances greater than 1 kpc, probably since their identification against the field becomes increasingly difficult. Cepheids, on the other hand, are detectable at much greater distances, thanks to their high luminosity and characteristic brightness variations.

However, a cluster's probability of hosting a Cepheid is governed by stellar evolution and star formation. For a given distribution of stellar masses, only a small fraction will become seen as Cepheids during their lifetime (stars with masses between  $\sim 4 - 11M_{\odot}$ ). Due to the nature of the IMF, these intermediate mass stars constitute a small fraction of the total number of cluster stars, and few such intermediate-mass stars are present in typical (small) open clusters. Furthermore, only a fraction (perhaps 10-20 %) of a suitable star's lifetime during the core Helium burning phase is spent on the blue loops, and even less within the instability strip. As a result, few CCs are known. The inverse problem of finding host clusters around known Cepheids (Turner et al. 1993; Turner 1998; Majaess et al. 2012b,d, e.g.), however, can be interesting, e.g. to constrain the survival rate of open clusters. Such studies can be very successful, see e.g. the "missing Combos" in Sec. 4.1.1 and the Cepheids belonging to OB associations listed in T10.

## 5.3 Implications for the Distance Scale

We are aware of the fact that our calibration, although performed on an 'optimal' set, remains inhomogeneous in the true distance moduli employed and the treatment of extinction. It is furthermore based on V-band data obtained in multiple different passbands with varying post processing techniques. These are the main limitations of the data employed. Furthermore, the number of CCs employed in the fit (18) is not very large, and the distance to NGC 7790 enters the fit three times, since its three CCs are included in the fit. Finally, the fit obtained is very sensitive to outliers, due to the lack of long-period calibrators.

We advocate that the 'optimal' sample presented, although incomplete (missing host clusters), forms an ideal sub-set for PLR calibrations, since all cluster memberships were self-consistently evaluated. However, to improve upon the calibration of the cluster-based PLR, two things would be particularly useful: a detailed homogeneous deep photometric study of the host clusters that includes careful treatment of extinction, and observational follow-up of the inconclusive CC candidates identified. Given the large discrepancies that are found between recent Galactic PLR calibrations (and their zero-points), such an observational campaign would be very desirable.

## 6 CONCLUSION

Focusing on Cepheids, we have performed an all-sky cluster membership census. Our analysis considers an up to 8-dimensional membership space that includes spatial and kinematic information, as well as parent population parameters (age, iron abundance). Although in some ways limited by data inhomogeneity and incompleteness, we identify 23 *bona fide* cluster Cepheids, including most canonical CCs accessible within our sample, as well as 5 new ones, and multiple additional CC candidates of interest.

The newly identified CCs are: SX Car in ASCC 61, S Mus in ASCC 69, UW Car in Collinder 220, ASAS J182714-1507.1 in Kharchenko 3 (fundamental-mode pulsators), and V379 Cas in NGC 129 (overtone pulsator). The cluster membership of these candidates must have escaped previous discovery, since most of the host clusters are not very well studied, and the Cepheids are located outside the cluster cores, cf. Sec. 4.2.

Since we can rank candidates according to membership probabilities, we consider our *bona-fide* CC sample ideal for calibrating the Galactic Cepheid PLR. However, data inhomogeneity, large uncertainties on cluster parameters, and a lack of long-period calibrators unfortunately limit the precision of the calibration we perform. We therefore highlight the need for observational campaigns dedicated to the host clusters of our *bona-fide* CC sample, as well as other interesting CC candidates identified.

The limitations that our work suffers due to inhomogeneous and incomplete data will be significantly reduced in the near future, thanks to the Gaia space mission. Specifically, Gaia will improve our study in the following ways:

- Thousands of new Cepheids (Eyer & Cuypers 2000; Windmark et al. 2011) will be discovered.
- Accurate absolute trigonometric parallaxes of Cepheids will become available up to distances of 6-12 kpc, depending on extinction (Eyer et al. 2012), thereby enabling a direct calibration of the Galactic period-luminosity-relationship similar to the one performed in the seminal paper by Feast & Catchpole (1997). This will remove our partial dependence on existing PLR calibrations when determining cluster membership. Accurate parallaxes to longer period Cepheids will also be obtained, thereby significantly improving the distance estimates to extragalactic Cepheids.
- The accuracy of proper motions will be improved by orders of magnitude, moving from  $\text{mas yr}^{-1}$  to tens of  $\mu\text{as yr}^{-1}$ , see Lindegren (2010) and the Gaia Science Performance website<sup>14</sup>.
- Homogeneous radial velocities (via the RVS instrument) and metallicity estimates (via the spectrophotometric instruments) will be available as membership constraints for a great number of Cepheids.
- Homogeneous metallicity estimates can be obtained through spectrophotometry-photometry (Liu et al. 2012).
- Thousands of new open clusters (ESA 2000) will be discovered, forming a more or less complete census of open clusters to distances up to 5 kpc. As was shown in Fig. 20, the distribution of Cepheids is still increasing at these distances.

<sup>14</sup> [http://www.rssd.esa.int/index.php?project=GAIA&page=Science\\_Performance#chapter1](http://www.rssd.esa.int/index.php?project=GAIA&page=Science_Performance#chapter1)

Hence, one may expect to find many more CCs in these parts of the Galaxy.

- Down to magnitude 20, all-sky homogeneous multi-epoch photometry and colors will be obtained that will include all the *bona-fide* cluster Cepheids mentioned in this work.

- Known clusters will be mapped in unprecedented detail, and intra-cluster dynamics will be accessible to determine membership.

Gaia's data homogeneity will significantly improve error budgets, since no offsets in instrumental zero-points (e.g. in RV) will have to be taken into account. The constraining power in terms of membership will thus be augmented considerably. Correlations between parameters, e.g. proper motion, parallax, and RV, can be determined self-consistently and accounted for (cf. van Leeuwen 2007). Such factors will make the Gaia era particularly exciting for work such as this.

## ACKNOWLEDGMENTS

Many heartfelt thanks to the observers who contributed to the Cepheid radial velocity campaigns, in particular to: Lovro Palaversa, Mihály Váradi, and Pierre Dubath. We gratefully acknowledge useful discussions with and comments received from Maria Süveges, Berry Holl, David G. Turner, Daniel Majaess, Laszlo Szabados, Imants Platais, Michael W. Feast, and the referee, C. David Laney; all of these helped to improve the manuscript.

This research has made use of: NASA's Astrophysics Data System Bibliographic Services; the SIMBAD database and VizieR catalogue access tool (cf. A&AS 143, 23), operated at CDS, Strasbourg, France; the International Variable Star Index (VSX) database, operated at AAVSO, Cambridge, Massachusetts, USA; the VO-tool TOPCAT<sup>15</sup>, see Taylor (2005); the WEBDA database, operated at the Institute for Astronomy of the University of Vienna; other online databases that provide Cepheid data, see article body.

## REFERENCES

- Akerlof C. et al., 2000, AJ, 119, 1901
- An D., Terndrup D. M., Pinsonneault M. H., 2007, ApJ, 671, 1640
- Anderson E., Francis C., 2012, Astronomy Letters, 38, 331, (XHIP)
- Anderson R. I., Eyer L., Mowlavi N., 2012, in IAU Symposium 285, Vol. 8, Advancing the Physics of Cosmic Distances, R. de Grijs, ed., pp. 275–277
- Andrievsky S. M., Bersier D., Kovtyukh V. V., Luck R. E., Maciel W. J., Lépine J. R. D., Beletsky Y. V., 2002a, A&A, 384, 140
- Andrievsky S. M. et al., 2002b, A&A, 381, 32
- Andrievsky S. M., Kovtyukh V. V., Luck R. E., Lépine J. R. D., Maciel W. J., Beletsky Y. V., 2002c, A&A, 392, 491
- Andrievsky S. M., Luck R. E., Kovtyukh V. V., 2005, AJ, 130, 1880
- Andrievsky S. M., Luck R. E., Martin P., Lépine J. R. D., 2004, A&A, 413, 159
- Arp H. C., 1958, ApJ, 128, 166
- Bakos G. Á., Lázár J., Papp I., Sári P., Green E. M., 2002, PASP, 114, 974
- Balona L. A., Laney C. D., 1995, MNRAS, 277, 250
- Baranne A. et al., 1996, A&AS, 119, 373
- Baranowski R. et al., 2009, MNRAS, 396, 2194
- Barnes, III T. G., Jeffery E. J., Montemayor T. J., Skillen I., 2005, ApJS, 156, 227
- Barnes, III T. G., Moffett T. J., Slovak M. H., 1987, ApJS, 65, 307
- Barnes, III T. G., Moffett T. J., Slovak M. H., 1988, ApJS, 66, 43
- Baumgardt H., Dettbarn C., Wielen R., 2000, A&AS, 146, 251
- Benedict G. F. et al., 2007, AJ, 133, 1810
- Berdnikov L. N., 2008, VizieR Online Catalog, II/285
- Berdnikov L. N., Dambis A. K., Vozyakova O. V., 2000, A&AS, 143, 211
- Bersier D., 2002, ApJS, 140, 465
- Bersier D., Burki G., Mayor M., Duquenois A., 1994, A&AS, 108, 25
- Bono G., Marconi M., Cassisi S., Caputo F., Gieren W. P., Pietrzynski G., 2005, ApJ, 621, 966
- Bukowiecki L., Maciejewski G., Konorski P., Strobel A., 2011, Acta Astron., 61, 231, (B11)
- Coulson I. M., Caldwell J. A. R., 1985, South African Astronomical Observatory Circular, 9, 5
- Coulson I. M., Caldwell J. A. R., Gieren W. P., 1985, ApJS, 57, 595
- Cutri R. M. et al., 2003, 2MASS All Sky Catalog of point sources. NASA/IPAC Infrared Science Archive
- Dias W. S., Alessi B. S., Moitinho A., Lépine J. R. D., 2002a, A&A, 389, 871, (D02)
- Dias W. S., Lépine J. R. D., Alessi B. S., 2001, A&A, 376, 441
- Dias W. S., Lépine J. R. D., Alessi B. S., 2002b, A&A, 388, 168
- Efremov Y. N., 1964, Peremennye Zvezdy, 15, 242
- Eggen O. J., 1980, IBVS, 1853, 1
- Eggen O. J., 1983, AJ, 88, 379
- ESA, 2000, Gaia: Composition, formation and evolution of the galaxy. Tech. rep., ESA-SCI(2000)4
- Evans N. R., 1983, ApJ, 272, 214
- Evans N. R., 1992, ApJ, 385, 680
- Evans N. R., Welch D. L., 1993, PASP, 105, 836
- Eyer L., Cuypers J., 2000, in Astronomical Society of the Pacific Conference Series, Vol. 203, IAU Colloq. 176: The Impact of Large-Scale Surveys on Pulsating Star Research, Szabados L., Kurtz D., eds., pp. 71–72
- Eyer L. et al., 2012, Ap&SS, 341, 207
- Feast M., 1999, PASP, 111, 775
- Feast M. W., 1957, MNRAS, 117, 193
- Feast M. W., Catchpole R. M., 1997, MNRAS, 286, L1
- Fernie J. D., Evans N. R., Beattie B., Seager S., 1995, IBVS, 4148, 1
- Flower P. J., 1978, ApJ, 224, 948
- Fouqué P. et al., 2007, A&A, 476, 73
- Francis S. P., 1989, AJ, 98, 888

<sup>15</sup> <http://www.star.bris.ac.uk/~mbt/topcat/>

- Freedman W. L. et al., 2001, *ApJ*, 553, 47
- Frinchaboy P. M., Majewski S. R., 2008, *AJ*, 136, 118
- Froebrich D., Scholz A., Raftery C. L., 2007, *MNRAS*, 374, 399
- Fry A. M., Carney B. W., 1997, *AJ*, 113, 1073
- Geffert M., Bonnefond P., Maintz G., Guibert J., 1996, *A&AS*, 118, 277
- Gieren W. P., 1981, *ApJS*, 46, 287
- Gieren W. P., 1985, *ApJ*, 295, 507
- Gieren W. P., Fouqué P., Gomez M. I., 1997, *ApJ*, 488, 74
- Gieren W. P., Matthews J. M., Moffett T. J., Barnes, III T. G., Frueh M. L., Szabados L., 1989, *AJ*, 98, 1672
- Gilmore G. et al., 2012, *The Messenger*, 147, 25
- Giridhar S., 1983, *Journal of Astrophysics and Astronomy*, 4, 75
- Gorynya N. A., Irmambetova T. R., Rastorguev A. S., Samus N. N., 1992, *Soviet Astronomy Letters*, 18, 316
- Gorynya N. A., Samus' N. N., Rastorguev A. S., Sachkov M. E., 1996, *Astronomy Letters*, 22, 175
- Gorynya N. A., Samus' N. N., Sachkov M. E., Rastorguev A. S., Glushkova E. V., Antipin S. V., 1998, *Astronomy Letters*, 24, 815
- Gorynya N. A., Samus N. N., Sachkov M. E., Rastorguev A. S., Glushkova E. V., Antipin S. V., 2002, *VizieR Online Data Catalog III/229*, 3229, 0
- Groenewegen M. A. T., 2008, *A&A*, 488, 25
- Groenewegen M. A. T., Romaniello M., Primas F., Mottini M., 2004, *A&A*, 420, 655
- Harris G. L. H., van den Bergh S., 1976, *ApJ*, 209, 130
- Hoyle F., Shanks T., Tanvir N. R., 2003, *MNRAS*, 345, 269
- Imbert M., 1999, *A&AS*, 140, 79
- Irwin J. B., 1955, *Monthly Notes of the Astronomical Society of South Africa*, 14, 38
- Jaynes E. T., 2003, *Probability Theory - The Logic of Science*. Cambridge University Press
- Kharchenko N. V., 2001, *Kinematika i Fizika Nebesnykh Tel*, 17, 409
- Kharchenko N. V., Piskunov A. E., Röser S., Schilbach E., Scholz R.-D., 2005a, *A&A*, 440, 403
- Kharchenko N. V., Piskunov A. E., Röser S., Schilbach E., Scholz R.-D., 2005b, *A&A*, 438, 1163, (K05)
- Kharchenko N. V., Piskunov A. E., Schilbach E., Röser S., Scholz R.-D., 2012, *A&A*, 543, A156, (K12)
- Kharchenko N. V., Scholz R.-D., Piskunov A. E., Röser S., Schilbach E., 2007, *AN*, 328, 889
- Kholopov P. N., 1956, *Peremennye Zvezdy*, 11, 325
- King I., 1962, *AJ*, 67, 471
- Kiss L. L., 1998, *MNRAS*, 297, 825
- Klagyivik P., Szabados L., 2009, *A&A*, 504, 959, (KS09)
- Kovtyukh V. V., Andrievsky S. M., Belik S. I., Luck R. E., 2005a, *AJ*, 129, 433
- Kovtyukh V. V., Soubiran C., Luck R. E., Turner D. G., Belik S. I., Andrievsky S. M., Chekhonadskikh F. A., 2008, *MNRAS*, 389, 1336
- Kovtyukh V. V., Wallerstein G., Andrievsky S. M., 2005b, *PASP*, 117, 1173
- Kukarkin B. V., Kholopov P. N., 1982, *New Catalogue of Suspected Variable Stars*. Moscow: Publication Office Nauka, 1982
- Laney C. D., Caldwell J. A. R., 2007, *MNRAS*, 377, 147
- Lasker B. M. et al., 2008, *AJ*, 136, 735
- Leavitt H. S., Pickering E. C., 1912, *Harvard College Observatory Circular*, 173, 1
- Lemasle B., François P., Bono G., Mottini M., Primas F., Romaniello M., 2007, *A&A*, 467, 283
- Lemasle B., François P., Piersimoni A., Pedicelli S., Bono G., Laney C. D., Primas F., Romaniello M., 2008, *A&A*, 490, 613
- Lindgren L., 2010, in *IAU Symposium 261*, Vol. 5, *Relativity in Fundamental Astronomy: Dynamics, Reference Frames, and Data Analysis*, S. A. Klioner P. K. S., Soffel M. H., eds., pp. 296–305
- Liu C., Bailer-Jones C. A. L., Sordo R., Vallenari A., Borraichero R., Luri X., Sartoretti P., 2012, *MNRAS*, 426, 2463
- Lloyd Evans T., 1980, *South African Astronomical Observatory Circular*, 1, 257
- Lovis C., Mayor M., 2007, *A&A*, 472, 657
- Luck R. E., Gieren W. P., Andrievsky S. M., Kovtyukh V. V., Fouqué P., Pont F., Kienle F., 2003, *A&A*, 401, 939
- Luck R. E., Lambert D. L., 2011, *AJ*, 142, 136
- Macri L. M., Stanek K. Z., Bersier D., Greenhill L. J., Reid M. J., 2006, *ApJ*, 652, 1133
- Majaess D., Turner D., Gieren W., 2012a, *ApJ*, 747, 145
- Majaess D., Turner D., Gieren W., Balam D., Lane D., 2012b, *ApJ*, 748, L9
- Majaess D. et al., 2011, *ApJ*, 741, L27
- Majaess D., Turner D. G., Gallo L., Gieren W., Bonatto C., Lane D. J., Balam D., Berdnikov L., 2012c, *ApJ*, 753, 144
- Majaess D., Turner D. G., Gieren W., 2012d, *MNRAS*, 421, 1040
- Majaess D. J., Turner D. G., Lane D. J., 2008, *MNRAS*, 390, 1539
- Matthews J. M., Gieren W. P., Mermilliod J.-C., Welch D. L., 1995, *AJ*, 110, 2280
- McSwain M. V., Gies D. R., 2005, *ApJS*, 161, 118
- Mermilliod J. C., 1988, *Bulletin d'Information du Centre de Données Stellaires*, 35, 77
- Mermilliod J.-C., 1995, in *Astrophysics and Space Science Library*, Vol. 203, *Information & On-Line Data in Astronomy*, Egret D., Albrecht M. A., eds., pp. 127–138
- Mermilliod J. C., Mayor M., Udry S., 2008, *A&A*, 485, 303
- Metzger M. R., Caldwell J. A. R., McCarthy J. K., Schechter P. J., 1991, *ApJS*, 76, 803
- Metzger M. R., Caldwell J. A. R., Schechter P. L., 1992, *AJ*, 103, 529
- Metzger M. R., Caldwell J. A. R., Schechter P. L., 1998, *AJ*, 115, 635
- Monson A. J., Pierce M. J., 2011, *ApJS*, 193, 12
- Mottini M., 2006, *Ph.D. Thesis*. Ludwig-Maximilians-Universität, München
- Perryman M. A. C., ESA, eds., 1997, *ESA Special Publication*, Vol. 1200, *The HIPPARCOS and TYCHO catalogues*. Astrometric and photometric star catalogues derived from the ESA HIPPARCOS Space Astrometry Mission
- Pettersson O. K. L., Cottrell P. L., Albrow M. D., Fokin A., 2005, *MNRAS*, 362, 1167
- Platais I., 1979, *Astronomicheskij Tsirkulyar*, 1049, 4
- Platais I., 1986, *Nauchnye Informatsii*, 61, 89
- Pojmanski G., 1997, *Acta Astron.*, 47, 467
- Pojmanski G., 2002, *Acta Astron.*, 52, 397



- Pojmanski G., Pilecki B., Szczygiel D., 2005, *Acta Astron.*, 55, 275
- Pont F., Burki G., Mayor M., 1994, *A&AS*, 105, 165
- Pont F., Queloz D., Bratschi P., Mayor M., 1997, *A&A*, 318, 416
- Queloz D. et al., 2001, *The Messenger*, 105, 1
- Queloz D. et al., 2000, *A&A*, 354, 99
- Raskin G. et al., 2011, *A&A*, 526, A69
- Rastorguev A. S., Glushkova E. V., Dambis A. K., Zabolotskikh M. V., 1999, *Astronomy Letters*, 25, 595
- Robichon N., Arenou F., Mermilliod J.-C., Turon C., 1999, *A&A*, 345, 471
- Roeser S., Demleitner M., Schilbach E., 2010, *AJ*, 139, 2440
- Romaniello M., Primas F., Mottini M., Groenewegen M., Bono G., François P., 2005, *A&A*, 429, L37
- Romaniello M. et al., 2008, *A&A*, 488, 731
- Samus N., Durlevich O., Kazarovets E. V., Kireeva N., Pastukhova E., Zharova A., et al., 2012, *General Catalog of Variable Stars (GCVS database, Version 2012Jan)*, available at the CDS as: B/gcvs or under <http://www.sai.msu.ru/gcvs/gcvs/>
- Sánchez N., Vicente B., Alfaro E. J., 2010, *A&A*, 510, A78
- Sandage A., 1958, *ApJ*, 128, 150
- Sandage A., Tammann G. A., 2006, *ARA&A*, 44, 93
- Sandage A., Tammann G. A., Saha A., Reindl B., Macchetto F. D., Panagia N., 2006, *ApJ*, 653, 843
- Schmidt E. G., 1982, *AJ*, 87, 1197
- Ségransan D. et al., 2010, *A&A*, 511, A45
- Soszynski I. et al., 2010, *Acta Astron.*, 60, 17
- Soszynski I. et al., 2008, *Acta Astron.*, 58, 163
- Storm J., Carney B. W., Gieren W. P., Fouqué P., Latham D. W., Fry A. M., 2004, *A&A*, 415, 531
- Storm J. et al., 2011, *A&A*, 534, A94
- Szabados L., 2003, *IBVS*, 5394, 1
- Szabados L. et al., 2013, *MNRAS*, 430, 2018
- Sziládi K., Vinkó J., Poretti E., Szabados L., Kun M., 2007, *A&A*, 473, 579
- Tadross A. L., 2008, *New Astronomy*, 13, 370
- Tammann G. A., Sandage A., Reindl B., 2003, *A&A*, 404, 423
- Taylor M. B., 2005, in *Astronomical Society of the Pacific Conference Series*, Vol. 347, *Astronomical Data Analysis Software and Systems XIV*, Shopbell P., Britton M., Ebert R., eds., p. 29
- Tsarevsky G. S., Ureche V., Efremov Y. N., 1966, *Astrophotomicheskij Tsirkulyar*, 367, 1
- Turner D. G., 1976, *AJ*, 81, 1125
- Turner D. G., 1977, *PASP*, 89, 277
- Turner D. G., 1980, *ApJ*, 240, 137
- Turner D. G., 1981, *AJ*, 86, 231
- Turner D. G., 1982, *PASP*, 94, 1003
- Turner D. G., 1986, *AJ*, 92, 111
- Turner D. G., 1992, *AJ*, 104, 1865
- Turner D. G., 1998, *AJ*, 116, 274
- Turner D. G., 2010, *Ap&SS*, 326, 219
- Turner D. G., Billings G. W., Berdnikov L. N., 2001, *PASP*, 113, 715
- Turner D. G., Burke J. F., 2002, *AJ*, 124, 2931
- Turner D. G. et al., 2008, *MNRAS*, 388, 444
- Turner D. G., Forbes D., Pedreros M., 1992, *AJ*, 104, 1132
- Turner D. G., Kovtyukh V. V., Usenko I. A., Gorlova N. I., 2013, *ApJ*, 762, L8
- Turner D. G. et al., 2012, *MNRAS*, 422, 2501
- Turner D. G., Majaess D. J., Lane D. J., Rosvick J. M., Henden A. A. B. D. D., 2010, *Odessa Astronomical Publications*, 23, 119
- Turner D. G., Mandushev G. I., Forbes D., 1994, *AJ*, 107, 1796
- Turner D. G., Mandushev G. I., Welch G. A., 1997, *AJ*, 113, 2104
- Turner D. G., Pedreros M., 1985, *AJ*, 90, 1231
- Turner D. G., Pedreros M. H., Walker A. R., 1998, *AJ*, 115, 1958
- Turner D. G., Usenko I. A., Kovtyukh V. V., 2006, *The Observatory*, 126, 207
- Turner D. G., van den Bergh S., Younger P. F., Danks T. A., Forbes D., 1993, *ApJS*, 85, 119
- Udalski A., Soszynski I., Szymanski M., Kubiak M., Pietrzynski G., Wozniak P., Zebrun K., 1999, *Acta Astron.*, 49, 223
- van den Bergh S., 1957, *ApJ*, 126, 323
- van Leeuwen F., ed., 2007, *Astrophysics and Space Science Library*, Vol. 350, *Hipparcos, the New Reduction of the Raw Data*. Springer
- van Leeuwen F., 2013, *A&A*, 550, L3
- Vazquez R. A., Feinstein A., 1990, *A&AS*, 86, 209
- Walker A. R., 1985a, *MNRAS*, 213, 889
- Walker A. R., 1985b, *MNRAS*, 214, 45
- Walker A. R., 1987, *MNRAS*, 229, 31
- Wilson T. D., Carter M. W., Barnes, III T. G., van Citters, Jr. G. W., Moffett T. J., 1989, *ApJS*, 69, 951
- Windmark F., Lindegren L., Hobbs D., 2011, *A&A*, 530, A76
- Woźniak P. R. et al., 2004, *AJ*, 127, 2436
- Yilmaz F., 1966, *Zeitschrift für Astrophysik*, 64, 54
- Yong D., Carney B. W., Teixeira de Almeida M. L., Pohl B. L., 2006, *AJ*, 131, 2256

## APPENDIX A: DETAILS ON INDIVIDUAL CLUSTER CEPHEID COMBINATIONS

### A1 Literature Combos

#### A1.1 Inconclusive Combos

**A1.1.1 CS Vel and Ruprecht 79** Membership of CS Vel in Ruprecht 79 was thoroughly discussed by Harris & van den Bergh (1976) who credited Tsarevsky et al. (1966) with first suggesting this particular combination. It has since been studied multiple times, e.g. by Walker (1987) and T10. Due to the sparse nature of the cluster, its reality as such was doubted by McSwain & Gies (2005), who conclude that Ruprecht 79 rather be a hole in the dust of the Sagittarius-Carina spiral arm than a physical open cluster.

None of the data from D02 are fully consistent with cluster membership for CS Vel, see Tab.1, and we calculate a likelihood of not even 1%, which contrasts the Cepheid's location inside  $r_c$ . The Cepheid's color excess from Laney & Caldwell (2007) agrees with the cluster value, however, and RV is not very far off. The cluster data from D02 and the uncertain existence of the cluster would suggest unlikely membership. However, the difficult parameter determination for this sparse cluster (candidate) means that only

a very detailed study of this region can reliably conclude on membership.

**A1.1.2 V1726 Cyg and Platais 1** V1726 Cyg’s membership results for Platais 1 are based on separation, proper motion, radial velocity, and age. The star was first considered for cluster membership by Platais (1979) and Turner et al. (1994), and is still often considered a *bona fide* member of Platais 1 (Turner et al. 2001, 2006). However, Platais (1986) concludes that the existence of this cluster is uncertain.

Of the membership constraints compiled, only proper motion does not significantly differ between cluster and Cepheid, although the magnitude of the Cepheid’s motion is a bit larger than that of the cluster. Radial velocity differs significantly, with the cluster receding more than  $10 \text{ km s}^{-1}$  faster than the Cepheid (Frinchaboy & Majewski 2008). In addition, the cluster’s age is significantly higher than the Cepheid’s. We do not calculate a PLR-based parallax, since V1726 Cyg may or may not be an overtone pulsator; the Fernie database places V1726 Cyg at approximately 2 kpc, while D02 list 1.3 kpc for Platais 1.

Unfortunately, there are great differences in cluster parameters to be found in the literature. For instance, K12 list 3.5 kpc as the cluster’s distance, which would exclude membership and be consistent with the higher proper motion of a foreground Cepheid. Interestingly, however, K12’s average cluster RV ( $-15.4 \text{ km s}^{-1}$ ) would agree with the Cepheid’s, although it is based on 21 stars in a poorly populated and supposedly distant (3.5 kpc in K12) cluster, rendering this estimate suspicious.

In summary, the constraints compiled here would tend to indicate non-membership. However, the significantly discrepant cluster distances and radial velocities from different references leave considerable doubt as to whether the cluster values adopted here are accurate. In light these issues and the possible non-existence of the cluster, we cannot conclude on membership of this Combo.

### A1.2 Unlikely Literature Combos

**A1.2.1 GH Car in Trumpler 18 or Hogg 12** Membership of the spectroscopic binary overtone pulsator GH Car (Szabados et al. 2013) in cluster Trumpler 18 was first proposed by Vazquez & Feinstein (1990) and then called into question by Baumgardt et al. (2000) who recommended radial velocity follow-up to draw a firmer conclusion. We compute a low likelihood of 14% based on proper motion, age, and RV. No parallax was calculated, since GH Car is an overtone pulsator. However, the Cepheid’s distance listed in the Fernie database (2.2 kpc) is significantly larger than Trumpler 18’s (1.4 kpc). Furthermore, the Cepheid is reddened by 0.1 mag more than the cluster, which is consistent with a greater distance to the Cepheid. The average cluster RV is based on the measurements of a single star, and does not agree with that of the Cepheid. In short, membership of GH Car in Trumpler 18 is unlikely.

However, our analysis identifies Hogg 12 as an alternative host cluster for GH Car. Based on proper motion and age, we compute a likelihood of 50% for this Combo. Proper motion is a very good match, and clearly detected. Finally,

reddening for the cluster and the Cepheid are nearly identical, and the Cepheid’s literature distance from the Fernie database matches the cluster’s distance very well. Follow-up is required to confirm this option.

**A1.2.2 SZ Tau and NGC 1647** The membership of SZ Tau in the halo of NGC 1647 was first considered by Efremov (1964) and later studied in more detail by Turner (1992) who concluded that SZ Tau is a ‘coronal’ member, based on star counts, reddening, radial velocity, proper motion from Francic (1989), and assuming overtone pulsation for SZ Tau.

From parallax (Storm et al. 2011), radial velocity, proper motion, and age, we compute a likelihood of 5%, the main discrepant constraints being radial velocity and proper motion from Tycho2 and Hipparcos (Dias et al. 2001; van Leeuwen 2007). The vanishing prior could, of course, be consistent with coronal membership. However, cluster membership based on proper motion was excluded by Geffert et al. (1996) using 2220 stars measured on photographic plates, and by Baumgardt et al. (2000) using Hipparcos proper motions. We therefore consider SZ Tau an unlikely member of NGC 1647, although an ejection cannot be excluded (Turner 2013, priv. comm.).

### A1.3 Non-member Combos discussed in the Literature

**A1.3.1 V442 Car and NGC 3496** V442 Car was previously considered for membership in NGC 3496 by Balona & Laney (1995) who concluded it to be a background star, based on age and reddening. From proper motion and separation, we come to the same conclusion. Furthermore, a rough distance estimate for a 14<sup>th</sup> magnitude 5.5 d Cepheid excludes membership in a cluster located approx. 1 kpc from the Sun.

**A1.3.2 UY Per and Czernik 8 or King 4** Turner (1977) suggested that UY Per could be a member of Czernik 8 or King 4. Turner et al. (2010) again mentions the latter combination. Our results, however, are inconsistent with membership in either cluster, based on the constraints parallax, proper motion, and age.

The ‘likelier’ of the two Combos is King 4, for which parallax and age are in relatively good agreement; the Cepheid is slightly farther away and has larger reddening. Kinetically, however, the cluster’s vanishing proper motion is inconsistent with membership of the rather fast moving Cepheid ( $\mu_{\alpha}^* = -6.15 \pm 2.8 \text{ mas yr}^{-1}$ ,  $\mu_{\delta} = 12.89 \pm 2.9 \text{ mas yr}^{-1}$ , PPMXL).

**A1.3.3 RCru, TCru and NGC 4349** The two Cepheids RCru and TCru have previously been considered as members of the open cluster NGC 4349 (Turner & Burke 2002), although they are no longer listed in Turner (2010). Our results are very clearly inconsistent with either Cepheid’s membership in this cluster. However, both Cepheids have very similar parallaxes and proper motions, and lie close to the open cluster Loden 624. Little information is available for this cluster, and observational follow-up is warranted.

**A1.3.4 TVCMa and NGC 2345** The membership constraints parallax, proper motion (vanishes), and age, agree within their respective uncertainties. The Cepheid's separation of 40' from cluster center results in a very low prior. Radial velocity differs by  $\sim 20 \text{ km s}^{-1}$  between cluster and Cepheid, resulting in a low likelihood. RV is the prime excluding constraint for this combo, and appears to be robust.

## A2 New Combos

In the following subsections, we discuss possible membership for selected Combos listed in Tab. 2. Observational follow-up is warranted for all the inconclusive Combos in the table, even if they are not discussed here in detail. Further information can be found in the data compiled that is available online, cf. Tab. A2. We furthermore remark that the ASAS targets in Tab. 2 are particularly worthy of follow up, since they have not yet received much attention.

### A2.1 Inconclusive Combos

**A2.1.1 Y Car and ASCC 60** Y Car is a double-mode Cepheid in a triple system with a B9.0V companion (Evans 1992) on a known orbit (see the Szabados 2003 binary Cepheids database<sup>16</sup>). The Cepheid lies well inside ASCC 60's projected core. Since the RV of the cluster in K05 was measured on a single star and is identical to Y Car's  $v_\gamma$ , we cannot consider this a valid membership constraint. Proper motion, on the other hand, is clearly measurable and consistent with membership. Reddening is slightly larger (by 0.07 mag) for the Cepheid than for the cluster, and the absolute magnitude of Y Car estimated by Evans (1992) indicates a distance modulus incompatible with that of the cluster, though we note that due to the sparsity of this cluster, a revised distance estimate would be useful. A detailed photometric and radial velocity study of ASCC 60 is required to conclude on the possible membership of Y Car. We furthermore note the presence of another Cepheid, CR Car inside ASCC 60's core radius. This Combo, however, is clearly inconsistent with membership. CR Car lies in the background of the cluster.

**A2.1.2 VZ CMa and Ruprecht 18** This combination yields a likelihood of 59 %, since metallicity and age are in excellent agreement between the cluster and the Cepheid. Proper motion is better discernible for the Cepheid than for the cluster, it seems, and color excess is 0.14 mag less strong for the Cepheid than for the cluster. According to D02, the cluster (1.1 kpc) lies bit closer than the Cepheid (1.3 kpc, from the Fernie database). In summary, both Cepheid and cluster require detailed follow-up for reddening and parallax, before we can conclude on the question of membership.

**A2.1.3 WZ Car and ASCC 63** Likelihood and prior both tend to clearly exclude WZ Car's membership in ASCC 63; the large projected distance from ASCC 63's core (33 pc assuming membership) lends further support to this

interpretation. However, the likelihood computed is completely dominated by the extreme mismatch in line-of-sight velocities ( $\delta v_{\text{rad}} = 120 \text{ km s}^{-1}$ ). Looking at the other constraints, however, we find that age, reddening, parallax (IRSB), and proper motion strongly suggest membership. Suspiciously, the cluster RV is based on only 2 stars, and may therefore not be reliable, or point towards an ejection event. We therefore judge this Combo inconclusive and stress the need for follow-up of the cluster.

### A2.2 Unlikely Combos

**A2.2.1 Y Sgr and IC 4725 (M25)** The parallaxes employed (Cepheid  $\varpi_{\text{Cep}} = 2.13 \pm 0.29$  from Benedict et al. 2007 and Cluster  $\varpi_{\text{Cl}} = 1.61 \pm 0.32$ ) in the calculation nearly agree within their respective error budgets. However, color excess is 0.3 mag lower for the Cepheid, which indicates that Y Sgr lies in the foreground of M 25.

Using the well-established cluster member U Sgr as a point of reference, we remark that proper motion, age, and metallicity are in excellent agreement between both Cepheids.  $v_\gamma$  differs slightly between the two, which could be explained by the known binarity of U Sgr and Y Sgr. The only significant discrepancy is in distance, which might be explained by uncertainties in extinction, since M 25 lies in the Orion arm (XHIP). However, we calculate a very low prior for this Combo, and if Y Sgr were a cluster member, it would lie at a large distance of 27 pc from cluster center. From these considerations, it appears that Y Sgr is an unlikely cluster member candidate.

**A2.2.2 BD+47 4225 (GSC 03642-02459) and Aveni-Hunter 1** The star was classified as a Cepheid based on HAT data by Bakos et al. (2002) with a light curve that suggests fundamental-mode pulsation. It lies barely outside  $r_c$  of cluster Aveni-Hunter 1. Unfortunately, proper motion and age are the only available membership constraints available in the literature compiled. Cluster and Cepheid appear to be co-moving in proper motion. Furthermore, the pulsational age of the Cepheid is spot-on with the cluster. However, a very rough distance estimate using the V-band magnitude (10.47) found in the Guide Star Catalog V. 2.3.2 (Lasker et al. 2008) yields a distance of 2.5 kpc for the Cepheid, which is 5 times the cluster distance. Since both objects are thus far not very well-studied, we highlight the need for follow-up of both cluster and Cepheid.

### A2.3 Non-members of interest

Non-member Combos of interest are listed in Tab. A1. We here present Combos with  $P(A) = 1$ , as well as others with high priors and information on parallax. Some of the Cepheids listed here belong to other open clusters, e.g. V Cen or X Cyg, or OB associations, e.g. S Vul (T10). Below, we discuss one of these cases, EY Car, since the membership probability computed is high.

**A2.3.1 EY Car and Alessi 5** The beat Cepheid EY Car lies within the core radius of Alessi 5. The available (kinematic only) membership constraints are consistent

<sup>16</sup> <http://www.konkoly.hu/CEP/intro.html>

**Table A1.** New Combos inconsistent with membership, despite high priors. Columns are described in Tab. 1.

Cluster	Cepheid	Constraints						$R_{cl}$ [pc]	$P(A)$	$P(B A)$	$P(A B)$
		$\varpi$	$v_r$	$\mu_\alpha^*$	$\mu_\delta$	[Fe/H]	age				
Alessi 5	EY Car	o	•	•	•	o	o	0.6	1.0	0.725	0.725
Koposov 12	CO Aur	o	o	$2.0\sigma$	$1.9\sigma$	o	o	3.5	1.0	0.023	0.023
Turner 1	S Vul	$2.8\sigma$	o	•	$1.6\sigma$	o	$1.3\sigma$	0.2	1.0*	0.015	0.015
NGC 5045	NSV 19655	o	o	$2.2\sigma$	$2.2\sigma$	o	o	1.8	1.0	0.008	0.008
Ruprecht 18	AO CMa	$3.8\sigma$	o	•	$1.4\sigma$	•	•	0.5	1.0	0.005	0.005
Collinder 173	AH Vel	o	o	o	o	$1.1\sigma$	$2.3\sigma$	11.8	1.0*	0.036	0.036
BH 34	ASAS J083130-4429.3	$3.9\sigma$	o	$1.6\sigma$	•	o	$2.7\sigma$	0.8	1.0*	0.0	0.0
ASCC 60	CR Car	$4.4\sigma$	$5.0\sigma$	$1.3\sigma$	•	o	$3.2\sigma$	0.7	1.0	0.0	0.0
Collinder 173	ASAS J080101-4543.6	o	o	o	o	o	$3.1\sigma$	5.3	1.0*	0.0	0.0
Collinder 65	V1256 Tau	$4.7\sigma$	o	•	$1.3\sigma$	o	$4.7\sigma$	3.4	1.0	0.0	0.0
Melotte 25	NSVS 9444700	o	o	o	o	o	$7.7\sigma$	1.2	1.0*	0.0	0.0
Stock 2	GL Cas	$4.7\sigma$	o	$5.3\sigma$	$7.6\sigma$	•	$1.4\sigma$	2.9	1.0	0.0	0.0
Turner 11	X Cyg	$3.4\sigma$	o	o	o	o	$5.2\sigma$	0.0	1.0*	0.0	0.0
Turner 7	V Cen	$5.0\sigma$	o	o	o	o	$15.5\sigma$	0.0	1.0*	0.0	0.0
King 7	V933 Per	o	o	•	$2.0\sigma$	o	$5.1\sigma$	3.4	1.0	0.0	0.0
NGC 6639	X Sct	$2.9\sigma$	$1.5\sigma$	•	$1.7\sigma$	o	$5.0\sigma$	1.2	0.853	0.0	0.0
Teutsch 14a	ASAS J180342-2211.0	$1.8\sigma$	o	o	o	o	$3.1\sigma$	2.2	0.814*	0.001	0.001
NGC 6873	ASAS J200829+2105.5	$4.5\sigma$	o	o	o	o	o	3.8	0.776*	0.0	0.0
SAI 94	SX Vel	$3.8\sigma$	o	o	o	o	$8.0\sigma$	4.2	0.761*	0.0	0.0
Collinder 240	FR Car	$2.8\sigma$	o	$2.2\sigma$	•	o	$1.5\sigma$	11.6	0.733*	0.005	0.004
NGC 6847	EZ Cyg	$2.4\sigma$	o	$1.2\sigma$	•	o	$5.4\sigma$	8.7	0.732*	0.0	0.0
BH 23	AT Pup	$3.5\sigma$	$2.6\sigma$	$1.2\sigma$	•	o	$2.9\sigma$	5.8	0.616*	0.0	0.0
Alessi-Teutsch 7	ASAS J082710-3825.9	$3.9\sigma$	o	$2.6\sigma$	•	o	•	17.8	0.59*	0.0	0.0
BH 164	AV Cir	$1.3\sigma$	$1.3\sigma$	$2.6\sigma$	$5.0\sigma$	o	•	9.1	0.572*	0.0	0.0
Czernik 43	PW Cas	$2.8\sigma$	o	•	•	o	$1.1\sigma$	2.4	0.565	0.044	0.025

with, but not very close to, each other. However, the literature distance from the Fernie database places the Cepheid nearly 2 kpc farther than the cluster, and the larger magnitude of proper motion is consistent with a foreground cluster. EY Car is thus not a cluster member, mentioned here only due to the high membership probability computed.

Cluster	Cepheid	R	P(A)	$P(B A)$	$P(A B)$	$\Delta\varpi$ $\sigma_{\varpi}$ Refs $_{\varpi}$	$\Delta v_r$ $\sigma_{v_r}$ Refs $_{v_r}$	$\Delta\mu_{\alpha}^*$ $\sigma_{\mu_{\alpha}^*}$ Refs $_{\mu_{\alpha}^*}$	$\Delta\mu_{\delta}$ $\sigma_{\mu_{\delta}}$ Refs $_{\mu_{\delta}}$	$\Delta[\text{Fe}/\text{H}]$ $\sigma_{[\text{Fe}/\text{H}]}$ Refs $_{[\text{Fe}/\text{H}]}$	$\Delta \log a$ $\sigma_{\log a}$ Refs $_{\log a}$
		RefR									
IC 4725	U Sgr	1.570	1.00000	0.98373	0.98373	-0.114 0.328	-0.090 3.606	-0.850 2.983	0.780 2.891	0.040 0.162	0.210 0.250
		K05				d,s,d,k,ks,V	MMB,*	t,h	d,ks		d,FU
NGC 7790	CF Cas	1.054	0.95454	0.97532	0.93098	0.056 0.070	0.399 3.606	-0.430 3.179	-0.090 2.410		-0.100 0.263
		B11				d,p,d,k,ks,G	MMU,*	BDW,h			d,FU
NGC 129	DL Cas	0.421	1.00000	0.85700	0.85700	0.063 0.127	-0.880 3.606	1.360 3.020	2.810 2.921		0.181 0.255
		K12				d,p,d,k,ks,G	MMU,*	t,h			d,FU
Turner 9	SU Cyg	0.067	1.00000	0.80743	0.80743	0.074 0.250	5.791 6.888	0.370 1.916	0.260 2.108		0.282 0.234
		K05				d,s,d,k,ks,G	K07,*	K05,h			d,FU
NGC 1647	SZ Tau	127.84	0.00000	0.04691	0.00000	0.060 0.376	-6.499 3.606	0.200 1.630	3.910 1.527		0.272 0.231
		K05				d,s,d,k,ks,G	MMU,*	t,h			d,FO
NGC 2345	TV CMa	38.208	0.00069	0.00001	0.00000	0.043 0.092	20.190 3.606	-0.720 1.836	1.290 2.208		-0.009 0.256
		B11				d,p,d,f,f,A	MMU,f	KHA,h			d,FU
NGC 4349	R Cru	14.985	0.04771	0.00000	0.00000	-0.717 0.106	1.308 3.606	4.790 2.280	2.510 2.229	-0.250 0.117	0.518 0.228
		K05				d,p,d,f,ks,b	MMU,*	BDW,h	d,l		d,FU
ASCC 61	SX Car	41.253	0.00056	0.91917	0.00051	0.042 0.122		2.060 2.985	0.950 2.480		0.110 0.250
		K05				d,p,d,f,ks,A		K05,h			d,FU
ASCC 69	S Mus	39.173	0.00446	0.87929	0.00392	-0.166 0.215	3.723 12.266	0.270 1.414	-0.040 1.807		0.260 0.253
		K05				d,s,d,fo,ks,**	K05,*	K05,h			d,FU
NGC 129	V379 Cas	42.900	0.00000	0.89594	0.00000		0.440 3.606	2.960 3.194	1.320 3.194		0.053 0.251
		K12					MMU,f	t,P			d,FO
ASCC 60	Y Car	1.228	1.00000	0.78642	0.78642		-2.100 7.985	-1.520 2.033	-0.850 1.291		
		K05					K07,*	K05,h			
... more data online ...											

**Table A2.** An excerpt of the data provided in the machine-readable online table. For each cluster-Cepheid combination we provide the parameters separation (R), prior, likelihood, and combined membership probability, as well as the differences between the individual membership constraints used (defined as cluster value minus Cepheid value), the combined error budgets adopted, and relevant references. For RefR, the cluster radius reference is provided. In column Refs $_{\varpi}$ , references are listed in the following order:  $\varpi_{\text{Cl}}$ ,  $\varpi_{\text{Cep}}$ ,  $E(\text{B}-\text{V})_{\text{Cl}}$ ,  $E(\text{B}-\text{V})_{\text{Cep}}$ , Cepheid  $\langle m_V \rangle$ , Cepheid period (the latter two are relevant if a PLR-based distance was used). For the remaining columns, two references are given; the first corresponds to the cluster, the second to the Cepheid. Due to spatial constraints, we abbreviate references in the following way: ‘a’ - values based on ASAS photometry, ‘b’ - values based on Berdnikov photometry, ‘d’ - Dias et al. (2002a) catalog, ‘f’ - Fernie database, ‘fo’ - Fouqué et al. (2007), ‘g’ - GCVS, ‘h’ - (van Leeuwen 2007), ‘k’ - Kovtyukh et al. (2008), ‘ks’ - Klagyivik & Szabados (2009), ‘l’ - Luck & Lambert (2011), ‘p’ - parallaxes computed from PLR-based distances, ‘P’ - PPMXL (Roeser et al. 2010), ‘s’ - Storm et al. (2011), ‘t’ - Dias et al. (2001, 2002b), ‘v’ - VSX, ‘\*’ - newly determined  $v_{\gamma}$  used, ‘\*\*’ - period improved using RV data, ‘B11’ - Bukowiecki et al. (2011), ‘FO’ - first overtone ages from Bono et al. (2005), ‘FU’ - fundamental mode ages from Bono et al. (2005), ‘K05’ - Kharchenko et al. (2005b,a), ‘K07’ - Kharchenko et al. (2007), ‘K12’ - Kharchenko et al. (2012), ‘MMB, MMU, BDW, KHA’ - see the references list in Dias et al. (2002a). The complete list of 3974 combinations can be retrieved from the online appendix to the paper.